**Atmospheric
Chemistry
and Physics**

Impact of aircraft NOx emissions on the atmosphere – tradeoffs to reduce the impact

M. Gauss[1], I. S. A. Isaksen[1], D. S. Lee[2], and O. A. Søvde[1]

[1]Department of Geosciences, University of Oslo, Oslo, Norway
[2]Manchester Metropolitan University, Manchester, UK

Abstract. Within the EU-project TRADEOFF, the impact of NOx (=NO+NO2) emissions from subsonic aviation upon the chemical composition of the atmosphere has been calculated with focus on changes in reactive nitrogen and ozone. We apply a 3-D chemical transport model that includes comprehensive chemistry for both the troposphere and the stratosphere and uses various aircraft emission scenarios developed during TRADEOFF for the year 2000. The environmental effects of enhanced air traffic along polar routes and of possible changes in cruising altitude are investigated, taking into account effects of flight route changes on fuel consumption and emissions.

In a reference case including both civil and military aircraft the model predicts aircraft-induced maximum increases of zonal-mean NOy (=total reactive nitrogen) between 156 pptv (August) and 322 pptv (May) in the tropopause region of the Northern Hemisphere. Resulting maximum increases in zonal-mean ozone vary between 3.1 ppbv in September and 7.7 ppbv in June.

Enhanced use of polar routes implies substantially larger zonal-mean ozone increases in high Northern latitudes during summer, while the effect is negligible in winter.

Lowering the flight altitude leads to smaller ozone increases in the lower stratosphere and upper troposphere, and to larger ozone increases at altitudes below. Regarding total ozone change, the degree of cancellation between these two effects depends on latitude and season, but annually and globally averaged the contribution from higher altitudes dominates, mainly due to washout of NOy in the troposphere, which weakens the tropospheric increase.

Raising flight altitudes increases the ozone burden both in the troposphere and the lower stratosphere, primarily due to a more efficient accumulation of pollutants in the stratosphere.

Correspondence to: M. Gauss
(michael.gauss@geo.uio.no)

1 Introduction

Driven mainly by continued economic growth and reduced fares, passenger traffic is estimated to grow at an average annual rate of nearly 5 percent during the period 2001–2020 (Airbus Global Market Forecast, 2002), making civil aviation one of the fastest growing industrial sectors. Emissions of aircraft include carbon dioxide (CO_2), water vapor (H_2O), nitric oxide (NO), nitrogen dioxide (NO_2), carbon monoxide (CO), a variety of hydrocarbons (HC), sulfur oxides, soot and other particles. Different aspects of the impact of aircraft emissions on the atmosphere have been identified, including changes in greenhouse gases, particles, contrails, and cirrus cloud formation (e.g. Fabian and Kärcher, 1997; Brasseur et al., 1998; Penner et al, 1999; Schumann et al., 2000; Isaksen et al., 2003). The main threat of aviation to the wider environment is believed to lie in its contribution to climate change.

The present study deals with the impact of NOx emissions from aircraft, which, although representing only 1–2% of the total emissions of NOx from man-made and natural sources in the early 1990s (Lee et al., 1997), may have a pronounced impact on the chemical composition of the atmosphere. During the last three decades numerous studies have focused on the different implications of NOx emissions from aircraft (e.g. Hidalgo and Crutzen, 1977; Johnson et al., 1992; Schumann et al., 1997; Dameris et al., 1998; Kentarchos and Roelofs, 2002, Grewe et al., 2002a, b). Most importantly, NOx emissions from aircraft are expected to increase ozone in the upper troposphere and lower stratosphere region (UTLS).

In contrast to all other major anthropogenic emission sources, aircraft emit their exhaust products directly into the UTLS, where pollutants have a much longer lifetime than at Earth's surface, allowing excess nitric oxide and ozone to accumulate to larger and more persistent perturbations than at Earth's surface. These factors, combined with the relatively

large radiative forcing caused by ozone increases occurring in the UTLS (Wang and Sze, 1980; Lacis et al., 1990; Hansen et al., 1997), make aircraft NO$_x$ emissions disproportionately important to the total O$_3$ radiative forcing from all sources. On the other hand, additional NO$_x$ and ozone enhance the concentration of the hydroxyl radical (OH), whereby the chemical lifetime of methane (CH$_4$) is reduced. The degree, to which the positive radiative forcing from ozone increases and the negative radiative forcing from methane reductions cancel each other, has long been under investigation (Penner et al., 1999). It is clear, however, that the two effects cannot be easily compared as they act on spatially and temporally different scales (Isaksen et al., 2001; Stevenson et al., 2004). Due to the relatively long lifetime of methane its aircraft-induced increases are well-mixed throughout the globe and exert radiative forcing mainly in low and mid latitudes. Ozone, on the other hand, is a short-lived greenhouse gas, with the largest perturbations and concomitant radiative forcing near the aircraft emission source in high northern latitudes.

The implication of NO$_x$ emissions for ozone levels depends strongly on the altitude of the emissions for both chemical and dynamical reasons. As aircraft emissions occur near the tropopause, only small shifts in flight altitude will lead to large changes in the fraction of emissions released into the stratosphere, where pollutants accumulate more efficiently due to less vertical mixing and the absence of washout processes. Secondly, the chemical production of ozone per emitted NO$_x$ molecule is a non-linear function of ambient levels of NO$_x$ (Brasseur et al., 1998; Jaeglé et al. 1998, 1999) and the availability of hydrocarbons (Brühl et al., 2000; Kentarchos and Roelofs, 2002), which in turn largely depend on altitude. In the sunlit troposphere and lower stratosphere, NO$_x$ leads to efficient ozone production through oxidation of carbon monoxide, methane, and higher hydrocarbons. At higher altitudes in the stratosphere this source becomes less important due the limited availability of hydrocarbons, while catalytic ozone depletion cycles involving NO$_x$ (Crutzen, 1970; Johnston, 1971) gain importance, and the injection of NO$_x$ actually destroys ozone rather than producing it.

The study presented in this paper has been performed within the EU-project TRADEOFF, funded by Framework Programme 5 of the European Commission. One of the main goals of TRADEOFF has been to study how the environmental impact of aircraft depends on flight routing and flight altitude. Model experiments using different aircraft emission scenarios were designed to provide an input for decision making on how to reduce aircraft impact in the future through change of air traffic patterns.

Here we present results contributed to TRADEOFF by the Oslo CTM-2 model, a three-dimensional global chemical transport model for the troposphere and the lower stratosphere. The particular strength of this model is the joint application of two comprehensive and well-tested chemistry schemes for the troposphere and the stratosphere, respec-

tively. This, combined with the use of a highly accurate advection scheme and a relatively high vertical resolution in the mid- to high-latitude tropopause region, makes the model suitable for assessing the impact of aircraft emissions. In the following section the model tool is briefly described, while Sect. 3 deals with the aircraft scenarios used in this study and their implementation in the Oslo CTM-2. A detailed presentation of results is given in Sect. 4, followed by conclusions and future directions in Sect. 5.

2   The Oslo CTM-2

All simulations presented in this paper have been performed with the Oslo CTM-2 model (hereafter "CTM2"), a global three-dimensional chemical transport model (CTM) for the troposphere and the lower stratosphere, driven by real meteorology from ECMWF (European Centre for Medium range Weather Forecasts). The CTM2 version focusing on tropospheric chemistry has been tested and applied in various papers (e.g. Bregman et al., 2001; Kraabøl et al., 2002; Grini et al., 2002; Isaksen et al., 2005), while the version including both tropospheric and stratospheric chemistry (used in this study) has so far been used in studies on the impact of water vapor emissions from aircraft (Gauss et al., 2003a) and radiative forcing due to past and future changes in tropospheric and lower stratospheric ozone (Gauss et al., 2003b, 2006). The model is run in 5.6×5.6 degrees horizontal resolution and with 40 sigma-pressure hybrid layers between the surface and 10 hPa. The vertical resolution in the tropopause region varies between about 0.8 km in high latitudes and about 1.2 km in low latitudes. Advective transport uses the highly-accurate and non-diffusive Second Order Moments scheme (Prather, 1986). Transport through deep convection is parameterized applying the Tiedtke mass flux scheme (Tiedtke, 1989), whereas boundary layer mixing is treated according to the Holtslag K-profile scheme (Holtslag et al., 1990). The calculation of dry deposition follows Wesely (1989), while wet deposition and washout are calculated based on the ECMWF data for convective activity, cloud fraction, and rainout and on the solubility of the species in question. Both large scale and convective washout processes are represented.

For the chemical integrations two comprehensive modules are used, which cover tropospheric and stratospheric chemistry, respectively. The tropospheric chemistry scheme calculates the evolution of 51 species taking into account 86 thermal reactions, 17 photolytic reactions, and 2 heterogeneous reactions. The module includes detailed hydrocarbon chemistry and has been thoroughly tested in the Oslo CTM-1 model (Berntsen and Isaksen, 1997). The stratospheric chemistry solver was developed by Stordal et al. (1985) and Isaksen et al. (1990) and has been extensively used and validated in a stratospheric 3-D CTM (Rummukainen et al., 1999). 158 reactions (104 thermal, 47 photolytic, and 7

heterogeneous) involving a total of 64 species (including 7 families) are integrated. In addition to the reactions that are relevant for the stratosphere the scheme includes the ozone production mechanism involving methane. The model version used in this study applies the scheme of Carslaw et al. (1995) to calculate rate coefficients for heterogeneous reactions occurring on sulfate aerosols and/or polar stratospheric clouds. Sulfate aerosol area densities are retrieved from SAGE satellite measurements for 1999. Both the tropospheric and stratospheric chemistry schemes apply the Quasi Steady State Approximation (QSSA) (Hesstvedt et al., 1978), using gas phase reactions rates from JPL evaluations (DeMore et al., 1997; Sander et al., 2000). Photodissociation rates are calculated on-line once every model hour applying the Fast-J2 method (Bian and Prather, 2002). The tropospheric and stratospheric chemistry modules are, respectively, called below and above the tropopause, which is defined and updated in the model every 6 h using tropopause pressures given by the NCEP (National Center for Environmental Prediction) reanalysis. It has to be stressed, however, that each transported species is present and advected throughout the entire model domain, and non-methane hydrocarbons are calculated above the tropopause according to their globally averaged stratospheric chemical lifetimes, so that no notable discontinuity exists at the transition zone between the two schemes. Anthropogenic emissions of source gases (CO, NO$_x$, Methane, VOC compounds) are the same as in the OxComp model intercomparison study of IPCC-TAR (Prather et al., 2001), based on an extrapolation of the EDGAR 2.0 database (Olivier et al., 1999) to year 2000 conditions. Natural emissions are taken from the Global Emissions Inventory Activity (GEIA, http://geiacenter.org) and Müller (1992). The lightning source is based on zonal-mean data given by Price et al. (1997a, b), scaled to a global output of to 5 Tg(N)/year. Monthly and zonally integrated emission are distributed among all grid cells and meteorological time steps based on local cloud top height and convective activity, following two formulas given by Price et al. (1997a) for continental and marine areas, respectively. The vertical distribution of lighting emissions within a column is computed following Pickering et al. (1998). Aircraft emissions are taken from TRADEOFF inventories as will be described in more detail in Sect. 3. The conversion of emitted NO$_x$ into HNO$_3$ and other nitrogen reservoir species within the aircraft plume is taken into account following the approach of Kraabøl et al. (2002) using the NILU aircraft plume model (Kraabøl et al., 1999).

The model has been evaluated in a number of earlier publications dealing with different chemical components (e.g. Brunner et al., 2003, 2005; Gauss et al., 2003a; Isaksen et al., 2005; Stevenson et al., 2006). Especially relevant in this context are the Brunner et al. (2003, 2005) papers, where the model (labeled there as "CTM2-Gauss" to distinguish from the version including tropospheric chemistry only) and other atmospheric models were compared to observational data from a number of research aircraft measurement campaigns. Trace gas fields simulated in the UTLS region were interpolated to the exact times and positions of the observations, allowing for a rigorous "point-by-point" evaluation of the models. Regarding ozone and NO$_x$ the outcome was positive in general, although differences were detected, such as an overestimation of NO$_x$ during winter in high latitudes and of ozone in the upper troposphere. Nevertheless, we are confident that CTM2 represents the state of the art in terms of aircraft impact studies focusing on chemical perturbations only.

3 Experimental setup

The main characteristics of the 9 model simulations discussed in this paper are summarized in Table 1. The aircraft emission scenarios were created for TRADEOFF for the year 2000 using the "FAST" (Future Aviation emissions Scenario Tool) model, developed especially for the purpose of the TRADEOFF studies. FAST calculates global inventories of fuel burnt, NO$_x$ emissions, and flown distances on a global grid, which is variable in horizontal and vertical dimensions as a user-specified input. The calculation methodologies and air traffic movement database were similar to those used for the ANCAT/EC inventory (Gardner et al., 1997) and identical to those used in the ANCTAT/EC2 inventory (Gardner et al., 1998), which was reviewed by Henderson et al. (1999). Aircraft were modeled using 16 types and engines, representative of the global fleet. Fuel-flow data for these 16 types were modeled using the same load factor assumptions as in ANCAT/EC2 (i.e. 85%) for a number of mission distances and specified cruise altitudes. The analysis of real mission data from the Eurocontrol and FAA (Federal Aviation Administration) air-space domains, using approximately 53 000 flights, revealed that cruise altitudes correlate with mission distances for the representative aircraft types. In the TRADEOFF scenarios cruise altitudes were prescribed on the basis of this analysis. As the movements database was for 1991/92, a scaling exercise was undertaken to create a year 2000 inventory. The performance of the aircraft fleet was changed according to historical trends in fuel efficiency, which was assumed to be 1.1% improvement per year. The growth in traffic fleet and revenue passenger kilometers between 1992 and 2000 was calculated based on FESG (Forecasting and Economic Support Group) projections (FESG, 1998; Penner et al., 1999) for the IS92f scenario (Leggett et al., 1992), as this scenario closely matches year 2000 ICAO (International Civil Aviation Organization) traffic data.

All TRADEOFF scenarios are provided on a 1°×1° horizontal grid with a vertical interval chosen on the same basis as the real data (i.e. flight level intervals of 2000 feet or 610 m), for 4 different seasons (December to February, March to May, June to August, and September to November). Aircraft NO$_x$ emissions are judged by an emission

Table 1. Summary of the model simulations and TRADEOFF aircraft emission scenarios.

Model run acronym	Aircraft emission scenario used	Fuel burn Tg/year	Total nitrogen emission [1] Tg(N)/year	E.I.(NO_x) [2] fleet average
no_air	no aircraft	–	–	–
ref	reference case including military aircraft movements	169.0	0.656 (15.6%)	12.7
base	base case	152.0	0.594 (16.9%)	12.9
pol_norm	additional polar routes, normalized [3]	152.0	0.594 (34.1%)	12.9
pol_adj	additional polar routes, adjusted fuel burn [3]	204.0	0.855 (34.1%)	13.8
low_norm	lower cruise altitude (–6000 ft), normalized [3]	152.0	0.594 (5.8%)	12.9
low_adj	lower cruise altitude (–6000 ft), adjusted fuel burn [3]	160.8	0.620 (5.8%)	12.7
high_norm	higher cruise altitude (+2000 ft), normalized [3]	152.0	0.594 (20.0%)	12.9
high_adj	higher cruise altitude (+2000 ft), adjusted fuel burn [3]	151.2	0.604 (20.0%)	13.1

1) The fraction of aircraft emissions occurring in the stratosphere is given in parenthesis (see Sect. 4.2).
2) The NO_x emission index, E.I.(NO_x), is defined as grams of NO_x (as NO_2) emitted per kg of burnt fuel.
3) Changes in flight routing will in general imply changes in fuel burn. In the "adjusted fuel burn" cases this effect is taken into account, while the "normalized" scenarios use the same total fuel burn as in the "base" case.
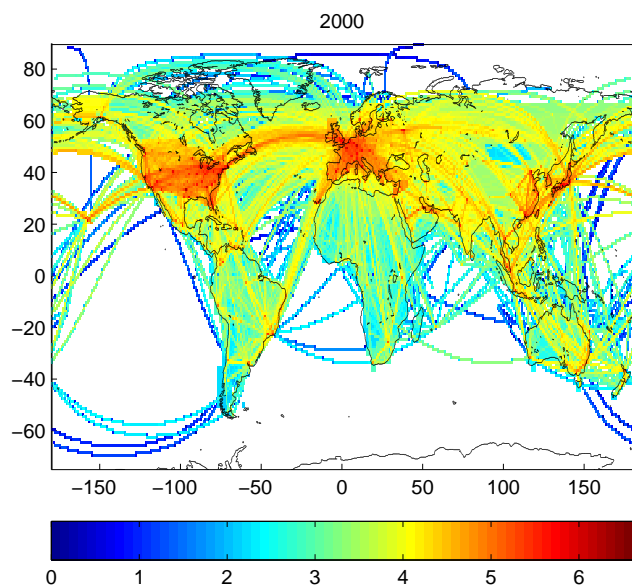

Fig. 1. Geographical distribution of aviation fuel burn in the TRADEOFF reference case (year 2000), vertically integrated for each $1° \times 1°$ column. Unit: $\log_{10}$[kg(fuel)/(day*$1° \times 1°$ column)].

index, E.I.(NO_x), equal to grams of NO_x (as NO_2) in the exhaust per kilograms of fuel burned. In the TRADEOFF reference case for the year 2000, which is used in model run "ref" (see Table 1), both civil and military aircraft are included with a global annual fuel consumption of about 169 Tg and a global annual nitrogen emission of 0.656 Tg(N)/year, corresponding to an average E.I.(NO_x) of 12.7. The geographical distribution of the annual fuel consumption according to this scenario is plotted in Fig. 1, revealing peak emissions in the North Atlantic Flight Corridor, in North America, Europe and the Far East. Using the NCEP tropopause height in

CTM2, about 16% of the global annual NO_x output from aviation is deposited directly into the stratosphere. However, this fraction is strongly dependent on season and latitude due to variations in tropopause height. At low latitudes, where the tropopause is high, aircraft operations occur entirely within the troposphere, while at high latitudes nearly all aircraft emissions are injected into the stratosphere. In mid-latitudes the tropopause height tends to be higher during summer leading to a somewhat smaller fraction of stratospheric emissions than during winter. This in reasonable agreement with what was found by Gettelman et al. (1999), who used both dynamical and thermal tropopause definitions for their analysis of the direct deposition of subsonic aircraft emissions into the stratosphere.

The novelty for the TRADEOFF work was the creation of seven scenarios for the investigation of the impact of polar routes and differing cruise altitudes: One base case and six perturbation cases. In contrast to the reference scenario ("ref") these scenarios do not include military aircraft. In the TRADEOFF base case (labeled "base"), which corresponds to "ref" but excludes military aircraft, the global annual fuel consumption and nitrogen emission amount to about 152 Tg(fuel)/year and 0.594 Tg(N)/year. This dataset compares very well with more recent scenarios that were developed for the years 2000 and 2002, and also neglect military aircraft: 1) the "FAST-2000" inventory, which is based on actual flight movements of year 2000 and yields 152 Tg(fuel)/year and 0.618(N)/year, and 2) the AERO2K inventory, which represents year 2002 emissions and is used in the European Commission QUANTIFY Project. AERO2K yields 156 Tg(fuel)/year and 0.627 Tg(N)/year. Both inventories are described in Lee et al. (2005).

In two of the perturbation cases a selection of already existing polar routes was substantially enhanced in order to investigate the impact of increased polar routing. The first one

(model run "pol_norm") is normalized with respect to the "base" case, i.e. polar flights come as replacement of flights in lower latitudes and the global annual fuel burn and nitrogen emission are identical to those in the "base" case. In the second one (model run "pol_adj"), the enhanced polar routing comes in addition to conventional traffic, so that the global annual fuel consumption and nitrogen emission are substantially larger than in the "base" case. Also, the fraction of emissions occurring in the stratosphere is much larger in the polar route scenarios, reflecting the low tropopause height in high latitudes. The variation of E.I.(NO$_x$) seen in Table 1 is a "real" effect in the inventories. In case "pol_adj", the frequency of a small number of routes that goes near the pole (a particular subset of aircraft types) is magnified. By doing this, the overall inventory E.I.(NO$_x$) changes as a result of changing the "population" of aircraft in the inventory.

The four remaining scenarios addressed changes in cruising altitude. In order to represent increased and decreased flight altitudes, increments of real flight levels were chosen, i.e. +2000 feet and −6000 feet (+610 m and −1830 m, respectively). The altitude decreases were specified by aircraft type and by mission distance. For the altitude increase some aircraft types for particular mission distances could not perform the flight. Thus, for this latter case, shifts in altitude were made only when feasible.

In the scenarios used for model runs "low_norm" and "low_adj", the flight altitude is reduced. Again the first scenario features the same global annual fuel consumption and nitrogen emission as the "base" case, while in the second one, changes in fuel consumption and nitrogen emissions are taken into account. This approach reflects the impact resulting from alternative flight routing in a more realistic way than the normalized scenarios. Moreover, it allows for a separate calculation of the impacts of changed emission altitude on the one hand and the concomitant change in fuel consumption on the other. As today's cruise altitudes are determined by fuel efficiency considerations, a decrease of 6000 ft in cruise altitudes will lead to an increase in fuel consumption related to increased drag. Accordingly, the total NO$_x$ emission is slightly larger compared to the "base" case. A considerable reduction is seen in the fraction of emissions released into the stratosphere, which in this case amounts to only 5.8% compared to 16.9% in the "base" case.

Finally, the emission scenarios applied in model runs "high_norm" and "high_adj" address an altitude increase of 2000 ft (610 m). A 2000 feet altitude increase is calculated to lead to a decrease in fuel consumption by 0.5% (owing to reduced drag), but to an increase in NO$_x$ emission of 1.6%. This is due to the fact that those aircraft types that can fly 2000 feet higher have a higher average E.I.(NO$_x$) at this altitude. In model run "high_adj" these changes are taken into account, while in model run "high_norm" the global annual fuel consumption and nitrogen emission are the same as in the "base" case run. Figure 2 shows the vertical distribution of aircraft NO$_x$ emissions in the "base" case and the four sce-
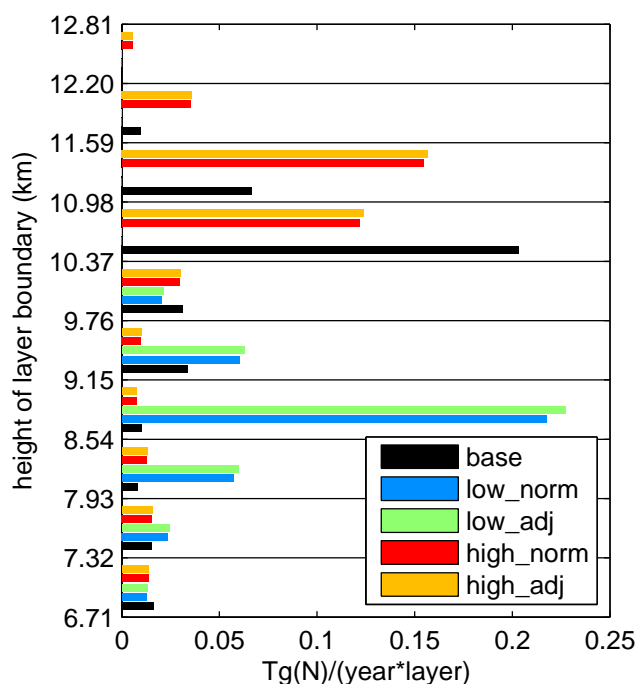

Fig. 2. Total annual NO$_x$ injection into flight levels between 6710 m and 12 810 m according to the TRADEOFF scenarios "base", "low_norm", "low_adj", "high_norm", and "high_adj" (see Table 1), plotted as Tg(N)/(year*610 m-layer). Thin horizontal lines depict flight level boundaries.

narios dealing with changes in flight altitude. As not all aircraft types are able to fly at higher altitudes the emissions in the altitude range with maximum "base" case traffic (10.37–10.98 km) is still large in the higher altitude scenarios, albeit reduced. By contrast, in the lower altitude scenarios no emissions occur in this region. The meteorology in all model simulations of this study is taken from ECMWF short-term (12–36 h) forecast data for the year 2000, which have been found to be better suited for the model than reanalyzed data. First, a five-year model spin-up is performed without aircraft to provide an initial condition for the 3-dimensional fields of all modeled chemical species. Starting from this initial condition, follow-up runs are integrated for three additional years without aircraft emissions and with aircraft emissions according to the various scenarios described above. The emissions and tropospheric boundary conditions used are summarized in Table 2. Surface emissions of CH$_4$ in the year 2000 are mimicked by setting a constant mixing ratio in the lowermost 5 layers of CTM2 (up to about 200 m). 1790 and 1700 ppbv are chosen in the Northern and Southern Hemispheres, respectively.

Table 2. Emissions and boundary conditions used in the model simulations.

Species	Mixing ratio/emission
CH$_4$	1745 ppbv
CO	547 Tg(CO)/year
VOC	133 Tg(C)/year
NO$_x$ – Biofuel	2.41 Tg(N)/year
NO$_x$ – Fossil Fuel	25.55 Tg(N)/year
NO$_x$ – Industry	2.01 Tg(N)/year
NO$_x$ – Biomass burning	5.84 Tg(N)/year
NO$_x$ – Soils	8.01 Tg(N)/year
NO$_x$ – Lightning	5.00 Tg(N)/year
NO$_x$ – Aircraft	0.59 – 0.71 Tg(N)/year (depending on scenario)
N$_2$O	318 ppbv
Cly (ETCL) [1]	3.54 ppbv
Bry (ETBL) [2]	16.34 pptv

1) Equivalent Tropospheric Chlorine Loading (WMO, 1999).
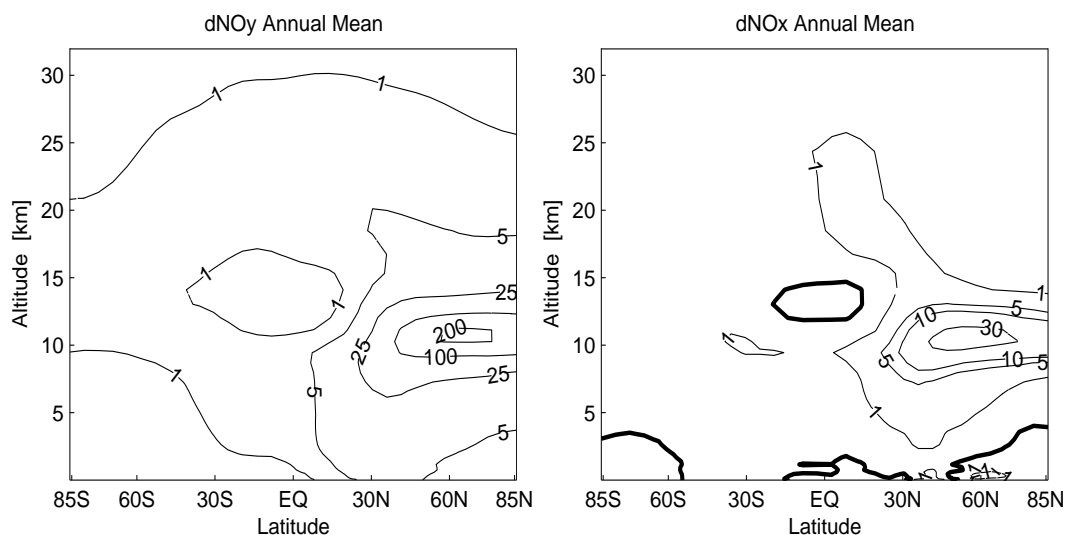2) Equivalent Tropospheric Bromine Loading (WMO, 1999).

Fig. 3. Annually averaged changes in zonal-mean NO$_y$ (left) and NO$_x$ (right) due to aircraft emissions in the TRADEOFF reference case, i.e. "ref minus no_air" (units: pptv). Contours at –1, 0, 1, 5, 25, 100, 200 for NO$_y$, and –1, 0, 1, 5, 10, 30 for NO$_x$.

4 Results

4.1 Impact of aircraft emissions in the tradeoff reference case

Model simulations "no_air" and "ref" are performed to assess the overall effect of NO$_x$ emissions from aircraft, including military aircraft. Figure 3 shows annually averaged zonal-mean changes in NO$_y$, i.e. total reactive nitrogen, defined as the sum of NO, NO$_2$, NO$_3$, N$_2$O$_5$, HNO$_4$, ClONO$_2$, BrONO$_2$, HNO$_3$, and PAN, and in NO$_x$, which is the sum of NO and NO$_2$, due to military and civil aircraft emissions in the year 2000. Notable perturbations are confined to the

Northern Hemisphere, reflecting the asymmetric distribution of aircraft emissions, with maximum increases amounting to 212 pptv for NO$_y$ and 45 pptv for NO$_x$. In CTM2 most of the NO$_y$ increase is present as HNO$_3$, as is apparent from the much smaller NO$_x$ increases. Small decreases of near-surface NO$_x$ are modeled in some areas, probably related to increases in ozone, which converts NO$_x$ into NOy as found in earlier aircraft studies (Stevenson et al. 1997). Regarding the seasonal variation and locations of the maximum perturbation (not shown), NO$_y$ is substantially enhanced during winter and spring with maximum increases between 250 and 300 pptv in the tropopause region in high Northern latitudes. In CTM2 this corresponds to a relative increase of about

Table 3. Changes in the total ozone column and, in parenthesis, the tropospheric ozone column, averaged over the globe and over the Northern Hemisphere in the various model simulations discussed in this and the following sections (units: DU). In order to obtain ozone burden change in Tg, global averages and Northern Hemisphere averages (in DU) have to be multiplied by 10.93 Tg/DU and 5.47 Tg/DU, respectively.

Model run accronym	Global average:		Northern Hemisphere average:	
	δ total ozone (DU) with respect to the "no_air" case	δ total ozone (DU) with respect to the "base" case	δ total ozone (DU) with respect to the "no_air" case	δ total ozone (DU) with respect to the "base" case
ref	+0.39 (+0.33)		+0.68 (+0.58)	
base	+0.34 (+0.29)		+0.59 (+0.50)	
pol_norm	+0.33 (+0.27)	−0.01 (−0.02)	+0.59 (+0.48)	+0.00 (−0.02)
pol_adj	+0.45 (+0.37)	+0.11 (+0.08)	+0.81 (+0.66)	+0.21 (+0.16)
low_norm	+0.31 (+0.29)	−0.03 (−0.00)	+0.55 (+0.50)	−0.04 (+0.00)
low_adj	+0.33 (+0.30)	−0.01 (+0.01)	+0.57 (+0.52)	−0.02 (+0.02)
high_norm	+0.35 (+0.29)	+0.01 (+0.00)	+0.60 (+0.50)	+0.01 (+0.00)
high_adj	+0.35 (+0.30)	+0.02 (+0.01)	+0.61 (+0.51)	+0.02 (+0.01)

40%. Throughout the year the maximum increase in zonal-mean NO$_y$ is located in mid- to high Northern latitudes between 10 and 12 km. During Northern Hemisphere Summer and in January the maximum increase is located at the North Pole (the northernmost latitude belt of CTM2 is centered at about 86 degrees N). In July and October the increases are almost twice as small but still pronounced. The seasonal variation of NO$_y$ perturbations is mainly related to meteorological conditions, in particular the height of the tropopause, which is low in high Northern latitudes during winter allowing aircraft emissions to accumulate more efficiently, and convective transport and washout of NO$_y$ in the troposphere. In particular during July, August, and September convective activity and thus vertical mixing and washout processes in the troposphere are relatively vigorous in CTM2 leading to smaller maximum increases in NO$_y$ at mid latitudes, as was already found in earlier CTM2 studies (Kraabøl et al., 2002). Thus the relatively smaller increase in high latitudes represents the maximum increase in NO$_y$ during these months. Maximum increases in NO$_x$ range from about 40 to almost 70 pptv, depending on season. At night and at large solar zenith angles, the NO$_x$/NO$_y$ ratio is low, leading to a notable displacement of the maximum NO$_x$ increase towards the equator during Northern Hemisphere winter.

The annual average of zonal-mean ozone and OH changes is shown in Fig. 4. The maximum increase in ozone is located in high Northern latitudes and amounts to 4.3 ppbv, while the maximum increase in OH is seen in mid Northern latitudes reaching 9.4×10^4 molecules cm^{-3}. Above about 20 km altitude in high southern latitudes ozone is slightly reduced through catalytic NO$_x$ cycles, although this perturbation is not pronounced. Regarding OH, NO$_x$ emissions lead to a slight enhancement through the reaction of NO and HO$_2$ and the increase of ozone, which is an OH precursor. Above a

certain height in the lower stratosphere, however, decreases in OH are modeled, albeit very small. This is probably connected to the reactions of HNO$_3$ and HO$_2$NO$_2$ with OH, which gain importance in the stratosphere in mid- to high latitudes in their competition with OH-producing reactions. The magnitude and latitude of the maximum ozone increase are plotted in Fig. 5. Owing to the close link between sunlight and ozone chemistry, the figure exhibits a strong seasonal variation. Maximum increases are seen during periods coinciding with low solar zenith angles, i.e. late spring and summer. The maximum is located in the northernmost latitude belt during summer, when the sun is present all day, while in winter it is displaced towards the equator, as far as 40 degrees North in the period December to February. The very high latitude of maximum increases during summer is explained by enhanced convective activity during summer, which reduces the ozone increase in mid-latitudes. Excess ozone produced from NO$_x$ emissions in the UTLS is transported into the lower troposphere where the chemical lifetime of ozone is shorter and where it is lost through dry deposition.

The maximum zonal-mean increase in ozone is modeled in June amounting to nearly 8 ppbv, coincident with maximum actinic flux. Relatively small ozone increases between 3 and 4 ppbv are modeled between September and January, resulting from a combination of less sunlight and lower NO$_y$ perturbations due to meteorological conditions.

Table 3 lists changes in total ozone for all perturbations discussed in this paper. For the increase due to aircraft in the TRADEOFF reference case ("ref") with respect to the "no_air" simulation a global mean increase of about 0.39 DU is modeled, corresponding to an ozone burden increase of 4.24 Tg. For the Northern Hemisphere these values are 0.68 DU and 3.72 Tg, i.e. most of the increase in ozone
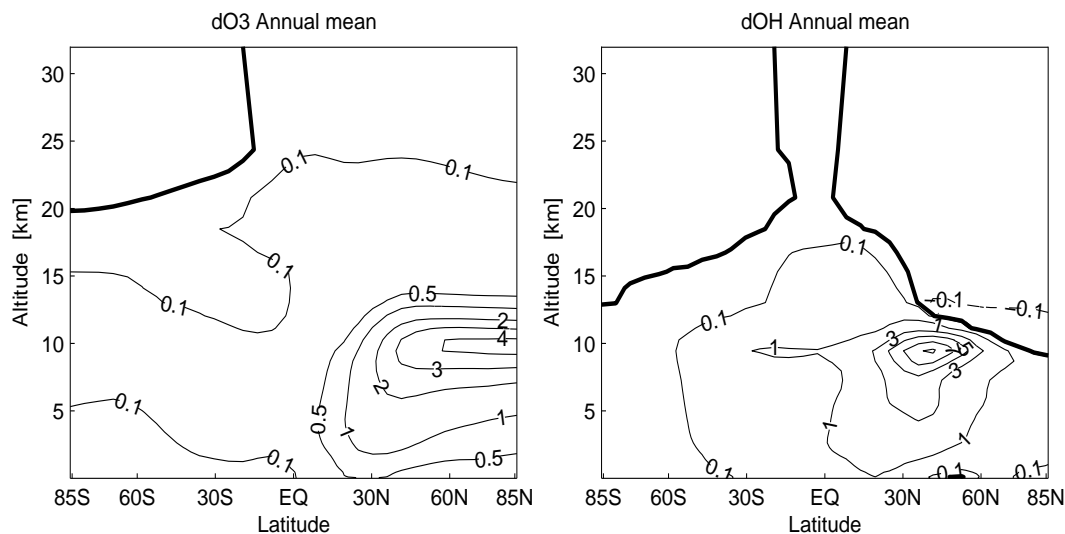
Fig. 4. Annually averaged changes in zonal-mean ozone (ppbv) and OH (10^4 molecules cm^{-3}) due to aircraft emissions in the TRADEOFF reference case, i.e. "ref minus no_air". Contours at: –0.1, 0, 0.1, 0.5, 1, 2, 3, 4 for ozone and –1, –0.1, 0, 0.1, 1, 3, 5, 7, 9 OH.
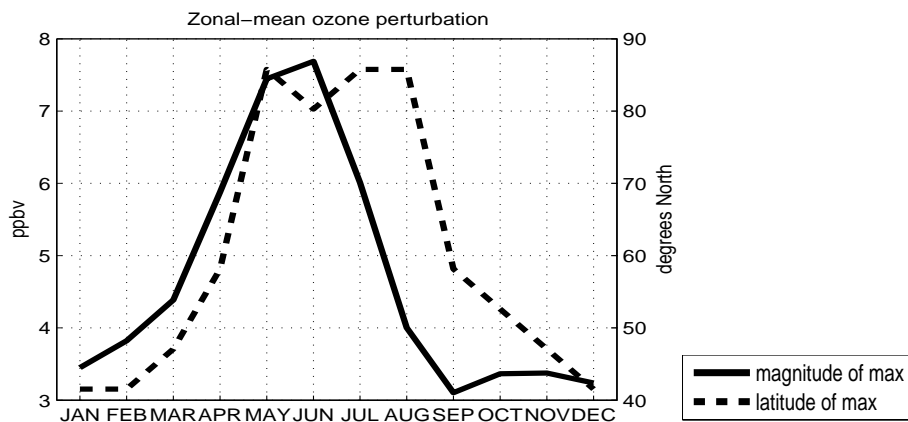

Fig. 5. Maximum increase in monthly averaged zonal-mean ozone due to aircraft in the TRADEOFF reference case as a function of season, i.e. "ref minus no_air". Solid line: magnitude of the maximum (ppbv, left axis), dashed line: latitude at which the maximum increase occurs (degrees North, right axis).

burden is located in the Northern Hemisphere. Values for changes in the tropospheric ozone column are listed in parenthesis. It is seen that most of the increase in the TRADEOFF reference case occurs in the troposphere. Concerning ozone column change, both the tropospheric and the total (i.e. surface to CTM2 lid) ozone columns are modeled to increase in all seasons and all latitudes. The maximum tropospheric and total column increases are modeled in mid- to high Northern Latitudes during May and amount to 1.15 DU (2.52%) and 1.34 DU (0.35%), respectively.

The results of this study can not easily be compared quantitatively with earlier studies, because new aircraft emission scenarios are used here. However, the spatial distribution and seasonal variation of NO$_x$ and ozone changes are similar to what was obtained in earlier studies (Wauben et al., 1997;

Stevenson et al., 1997; Berntsen and Isaksen, 1999; Kentarchos and Roelofs, 2002). Köhler et al. (1997) obtained maximum zonal-mean NO$_x$ increases exceeding 50 pptv in both January and July, i.e. somewhat larger than in the present study. This is due to the larger emission source used in their study (i.e. 0.85 Tg(N)/yr), but also to plume chemistry processes reducing both NO$_y$ and NO$_x$ perturbations in our study. Compared to the results of Kentarchos and Roelofs (2002), who used a total aircraft emission source of 0.56 Tg(N)/yr, our maximum ozone increase is further North in July and larger in magnitude, while the perturbations in NO$_x$ are in approximate agreement, especially in January (although it has to be noted that Kentarchos and Roelofs include HNO$_4$, NO$_3$ and N$_2$O$_5$ in the definition of their NO$_x$). In multi-model assessments such as in the IPCC special report
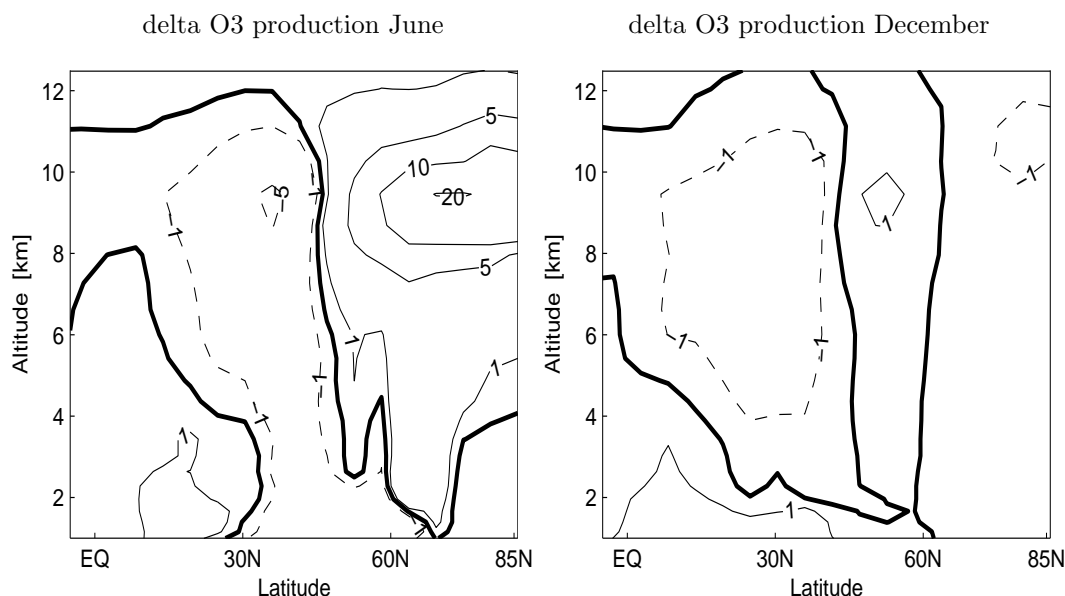
delta O3 production June

delta O3 production December

Fig. 6. Change in net chemical ozone production (10^3 molecules/cm^{-3}s^{-1}) due polar routes replacing conventional routes, i.e. "pol_norm minus base" in June (left) and December (right). Contours at –5, 1, 0, 1, 5, 10, and 20.

on Aviation and the Global Atmosphere (Penner et al., 1999) and the final report of the TRADEOFF project (Isaksen, 2003), uncertainties between the models concerning ozone change appear quite large, but the results obtained in our study are well within the uncertainty range of the modeling community. For example, in Penner et al. (1999, their Fig. 4-1) upper tropospheric ozone increases modeled for 2015 are typically in the range 5–10 ppbv, which compares well with the 4–5 ppbv obtained in our study, considering that the global aircraft NO$_x$ emission source is estimated about a factor of two smaller in 2000 (0.65 Tg(N)/year) than what was used in Penner et al. (1999) for 2015 (1.25 Tg(N)/year). The same is true for perturbations in NO$_x$, which amount to about 45 ppbv at maximum in our study (Fig. 3) compared to 60–150 ppbv in the IPCC (1999, their Fig. 4-2) models for 2015 using a doubled emission total. What is new in the present study with respect to IPCC (1999) is that we are using a model including both tropospheric and stratospheric chemistry, rather than prescribing stratospheric boundary conditions. In particular, both the ozone reducing effect from catalytic NO$_x$ cycles and the ozone producing effect of NO$_x$ emissions in the lower stratosphere are included in the our model stratosphere. The ozone depleting effect reveals itself in Fig. 4 in the Antarctic stratosphere, although this effect is negligible compared to the ozone producing effect of NO$_x$ emissions at lower altitudes.

4.2 Tradeoffs in enhanced polar routing

Six TRADEOFF scenarios were designed for comparison with the TRADEOFF base case ("base"), not including mili-

tary aircraft: two scenarios addressing polar routes and four dealing with changes in flight altitudes. The impact of aircraft emissions in the "base" case simulation is qualitatively the same as in the reference case ("ref"), which includes military aircraft and was discussed in the previous section. Due to the lower emission rate, however, the magnitudes of increase are slightly smaller, which is why the following discussion focuses on the relative change of aircraft impact due to flight routing rather than the aircraft impact itself.

In recent years polar routes in the Northern Hemisphere have been increasingly used by long range aircraft. For instance, great circle (i.e. shortest) connections between city pairs in Europe and the Western part of North America or between the Far East and the Eastern part of North America go through Arctic regions, and are/will be followed by airlines as closely as possible. Within TRADEOFF the impact of increased polar routing has been studied by enhancing already existing polar routes in the Northern Hemisphere significantly and by analyzing the model response. The polar environment differs from the mid-latitude regions because of the relatively low tropopause height, implying a larger fraction of the flight operations occurring in the stratosphere. This, in turn, implies a less efficient removal of NO$_x$ pollutants through wash-out at cruise altitudes. Also, the strong dependence of chemistry on sunlight combined with the strong seasonality of insolation in high latitudes lead to a large seasonal variability in ozone impact due to aircraft in high latitudes, which is of particular importance when considering increased high latitude routing. Figure 6 shows the change in net chemical production due to polar routing replacing standard routes. In June the impact is clearly revealed, while in
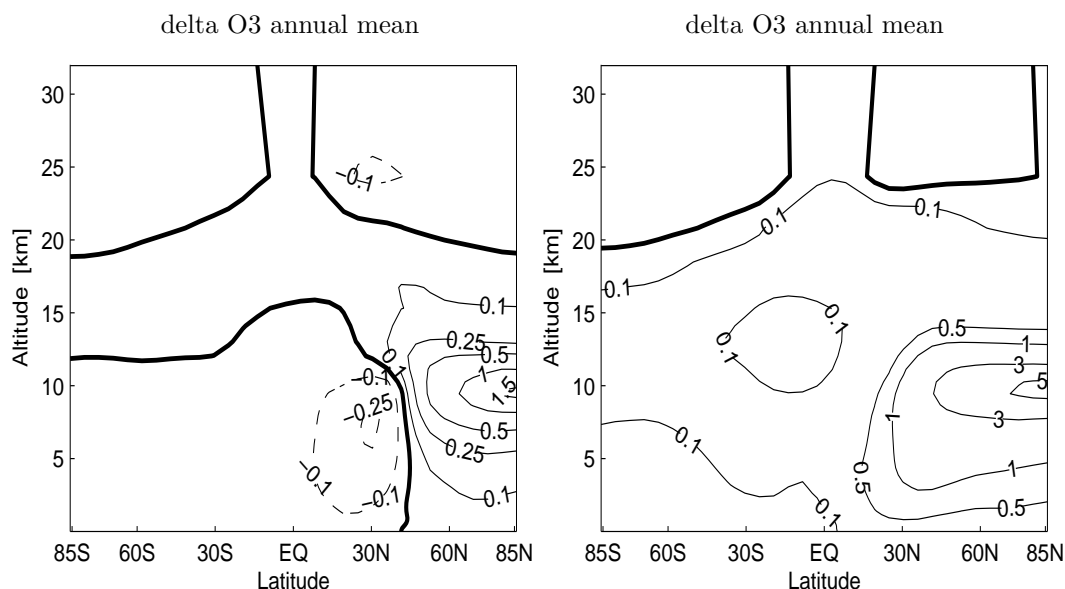
delta O3 annual mean   delta O3 annual mean

Fig. 7. Annually averaged zonal-mean ozone change (ppbv) due to polar routes replacing conventional routes (left panel, "pol_norm minus base") and the total impact due to aircraft emissions in the normalized polar route scenario (right panel, "pol_norm minus no_air"). Contours at −0.25, −0.1, 0, 0.1, 0.25, 0.5, 1, 1.5, 3, and 5 (in the right panel the 0.25 and 1.5 contours are omitted).

December in the absence of sunlight in high Northern latitudes, it is negligible. The slight decrease in mid-latitudes in this perturbation results from a reduction in mid-latitude traffic in this scenario. Annually averaged zonal-mean changes in ozone for the "pol_norm" simulation are presented in Fig. 7 with respect to the "base" and the "no_air" simulations. In the middle stratosphere signs of ozone depletion due to NO_x emissions are seen, but this effect is negligible in view of the large ambient ozone levels in these altitudes. The decrease of conventional routes manifests itself by the reduced ozone increase in mid- and low Northern latitudes in the troposphere with respect to the "base" case. The ozone impact with respect to the "no_air" case reveals appreciable increases in the Arctic up to an altitude of about 20 km. Maximum increases in the Arctic UTLS region with respect to the "no_air" simulation exceed 5 ppbv, which is more than 30% larger a perturbation than is obtained in the "base" case.

Figure 8 shows the seasonal variations of the maximum zonal-mean increases in NO_y and ozone, together with the global average increase in total ozone for the polar route scenarios (blue lines) and the other TRADEOFF scenarios to be discussed in Sect. 4.3 (red and green lines), along with the "base" case perturbation (black line). As shown by the blue lines in the upper panel of the figure, NO_y increases drastically in the polar route scenarios since washout of HNO_3 is less important in high latitudes and absent in the lower stratosphere, in which most of the additional high latitude emissions occur. The latitude of the maximum NO_y increase (not shown) is north of 80° N throughout the year. The maximum increase in zonal-mean ozone (blue line in the middle panel)

is strongly influenced by solar radiation, which is a maximum during summer. As the seasonal variation of actinic flux is particularly strong in high latitudes the seasonality of the maximum ozone increase is much more pronounced than in the "base" case. Indeed, in the normalized polar route scenario during winter, zonal mean increases in ozone are even smaller than in the "base" case. This is even more pronounced in the total ozone increase shown by the blue lines in the bottom panel of the figure. In the Northern Hemisphere, a replacement of conventional routes by polar routes would reduce the impact on the tropospheric column and increase the stratospheric column on an annual average since more emissions occur in the lower Arctic stratosphere. In the Southern Hemisphere both the increases in tropospheric and stratospheric columns are reduced with respect to the "base" case, as no high Southern latitude routes are introduced. Judging by the increase in global ozone burden only, a replacement of conventional routes by polar routes would reduce the environmental impact of aircraft with respect to the "base" case. However, this tradeoff is very small and subject to meteorological conditions such as washout and tropopause height in the Arctic regions, which are subject to interannual variation.

Concerning ozone column change due to polar routing replacing standard routes ("pol_norm minus base"), the aircraft-induced increase in both tropospheric and total ozone columns is reduced in low Northern latitudes due to the poleward shift of aircraft emissions. Substantial increases are confined to the summer season in high Northern latitudes. Regarding the ozone burden, the increases in ozone in high latitudes are not compensated by reductions in mid- and low
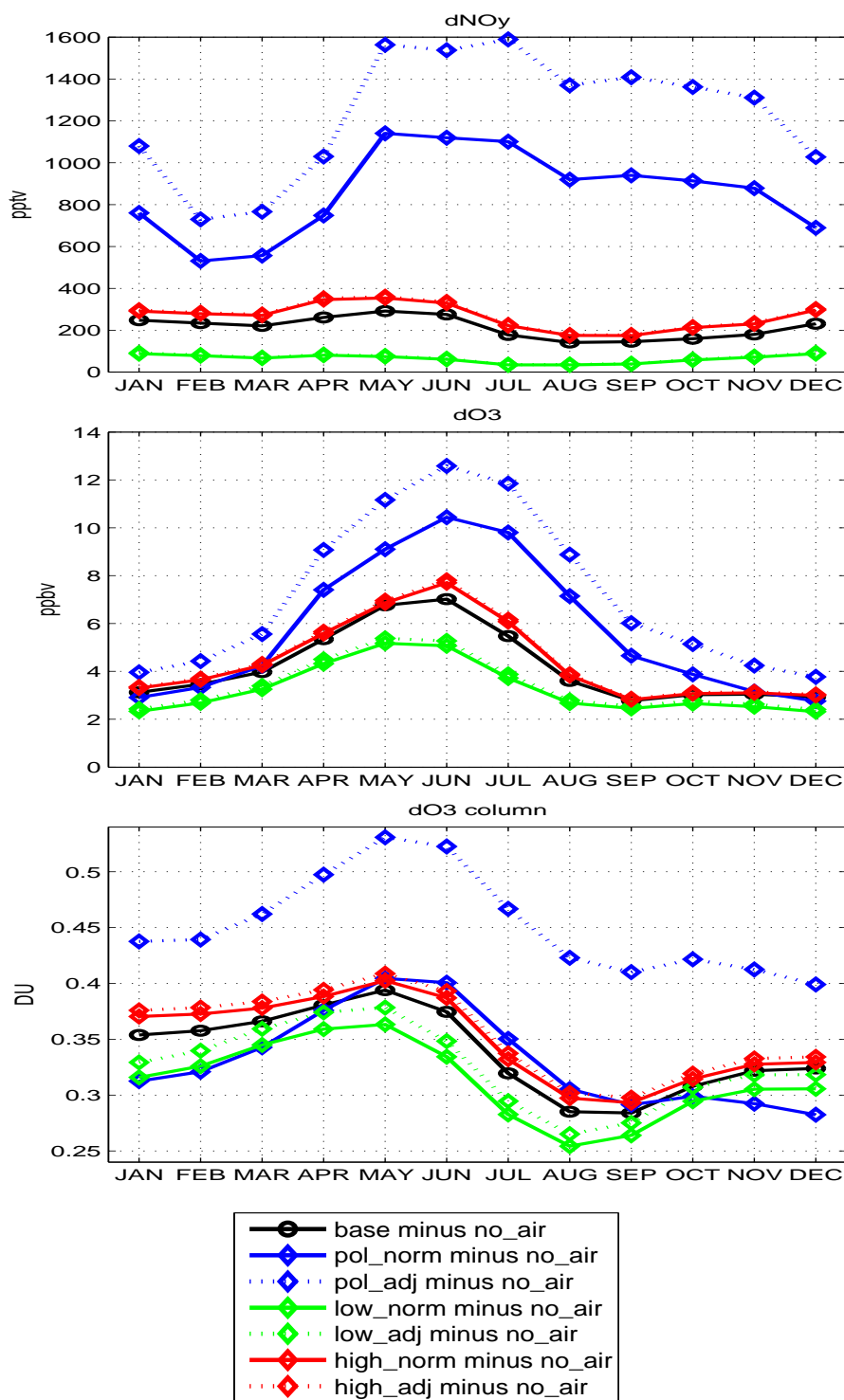
Fig. 8. Maximum zonal-mean NO$_y$ increase (upper panel, pptv), maximum zonal-mean ozone increase (middle panel, ppbv), and globally averaged ozone column increase (bottom panel, DU) as a function of season for different TRADEOFF simulations with respect to the "no_air" run.
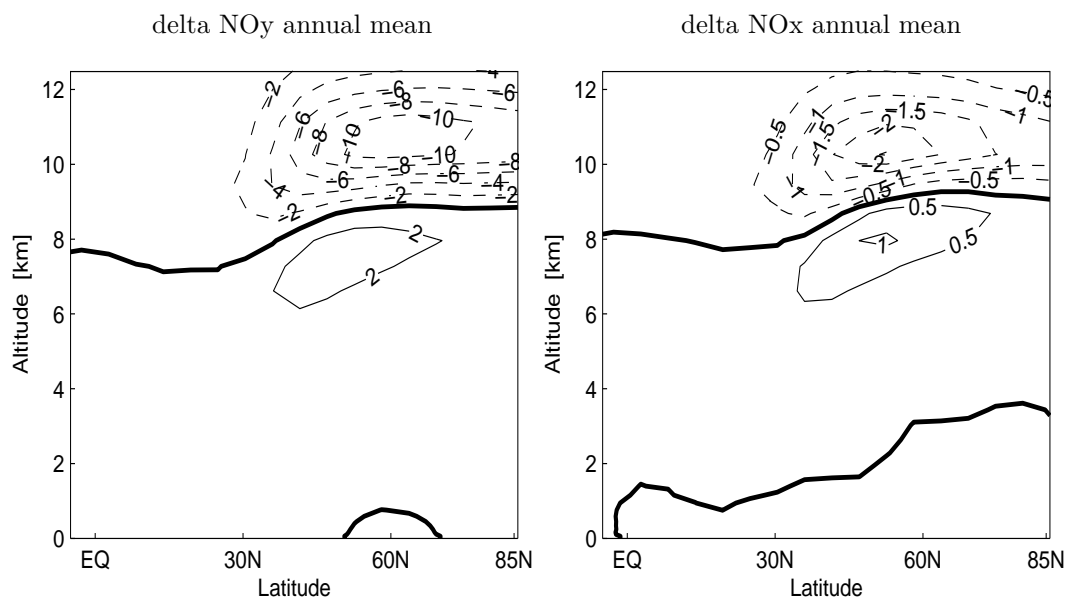
delta NOy annual mean

delta NOx annual mean

Fig. 9. Annual-mean changes in concentrations of NO$_y$ (top left, 10^8 molecules/cm^{-3}) and NO$_x$ (top right, 10^8 molecules/cm^{-3}) in the Northern Hemisphere due to a 1830 m reduction in flight altitude taking into account changes in fuel consumption, i.e. "low_adj minus base". Contours at –12, –10, –8, –6, –4, –2, 0, 2 for NO$_y$ and –2.5, –2, –1.5, –1, –0.5, 0, 0.5, 1 for NO$_x$.
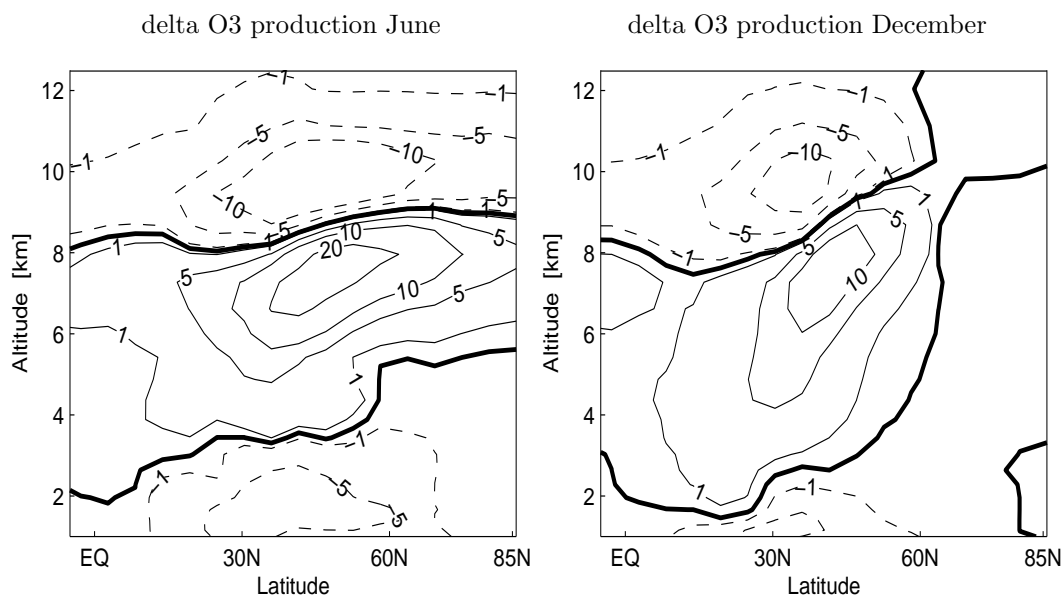
delta O3 production June

delta O3 production December

Fig. 10. Change in net chemical ozone production (10^3 molecules cm^{-3}s^{-1}) due to a 1830 m reduction in flight altitude, taking into account changes in fuel consumption, i.e. "low_adj minus base" in June (left) and December (right). Contours at –20, –10, –5, –1, 0, 1, 5, 10, and 20.

latitudes. With respect to the "no_air" case, the increase in ozone burden in the "pol_norm" scenario is thus substantially larger than in the "base" case.

4.3 Tradeoffs in changing flight altitude

Since the effects of aircraft NO$_x$ emissions exhibit strong altitudinal dependencies, it has been suggested that the air-

craft impact can be reduced by changing flight altitude. Changes in flight altitude will generally lead to modifications in the height profile of ozone change, with the impact getting smaller in certain height regions and larger in others. This is partly a direct consequence of changed distributions of aircraft emissions, but is also connected to the changes in the ambient conditions where the flights are operated. In
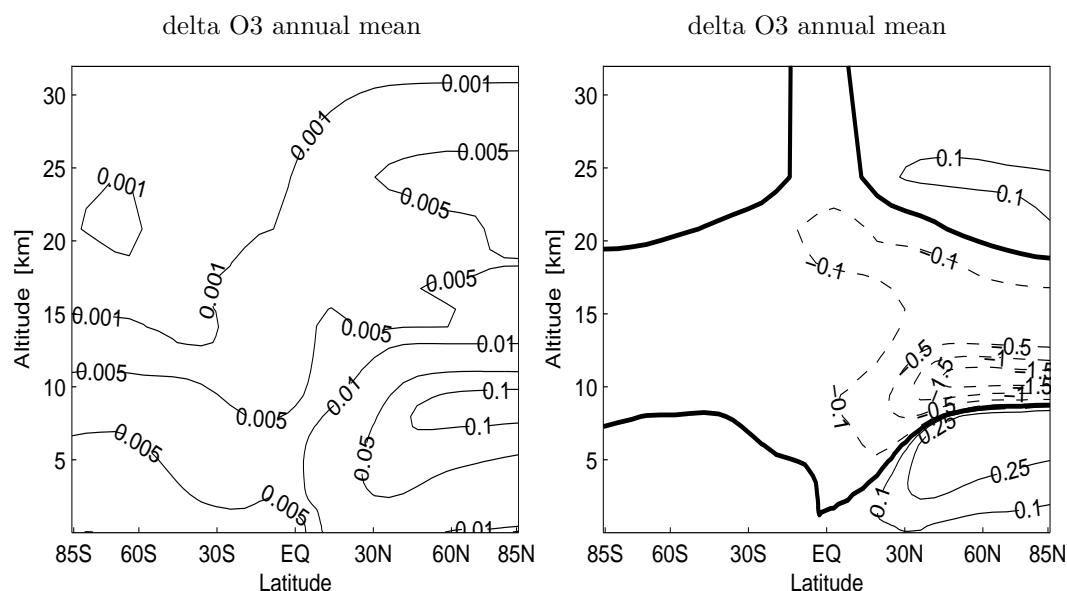
Fig. 11. Annually averaged zonal-mean ozone change (ppbv) due a 1830 m reduction in flight altitude. Left panel: "low_adj minus low_norm", i.e. separated effect of changes in fuel consumption, and right panel: "low_adj minus base", i.e. total effect of lowering the flight altitude.

particular, a higher cruise altitude will lead to a larger fraction of aircraft emissions occurring in the stratosphere where wash-out processes are largely absent and vertical motions are much slower. Thus NO$_x$ pollutants from aircraft can accumulate more efficiently leading to larger ozone perturbations. On the other hand ozone perturbations at lower altitudes become smaller as air traffic is reduced there. For the lower altitude scenarios the opposite is true. The key question to be addressed in this section is to what extent the negative and positive effects cancel each other in terms of total ozone column change.

Not surprisingly, lowering the flight altitude reduces aircraft impact at standard flight altitudes, while increasing it at lower altitudes. Figure 9 shows the zonal-mean change in the concentrations of NO$_y$ and NO$_x$ due to a 1830 m reduction in flight altitude taking into account changes in fuel consumption. In low to mid-Northern latitudes, we calculate decreases above 8 to 9 km altitude and increases below, which is a result of lowering the emission source. However, it is important to note that the increase at low altitudes is much smaller in magnitude than the decrease at high altitudes, although the increase in fuel consumption leads to a somewhat larger emission rate at the new altitude (the Figure shows changes in concentration rather than mixing ratios in order to make this relation clearer). In the case of NO$_y$, maximum reductions are modeled between 10 and 11 km altitude in Northern mid-latitudes, amounting to -11×10^8 molecules/cm^3, while the maximum increase between 6 and 8 km altitude remains below $+3 \times 10^8$ molecules/cm^3. For NO$_x$ the correspond-

ing maximum changes are -2.5×10^8 and $+1.1 \times 10^8$, respectively. This asymmetry is, first and foremost, connected to washout of HNO$_3$, which is much more efficient at low altitudes, while being virtually absent in the lower stratosphere. The HO$_x$ partitioning (not shown) is shifted towards OH in regions of enhanced NO$_x$ emissions, and towards HO$_2$ in regions of reduced NO$_x$ emissions. In low latitudes, increases in HO$_2$ are seen in the troposphere as well. These are regions where HO$_x$ increases as a whole due to the ozone increase. As a result of these changes, the ozone net production, shown in Fig. 10, is enhanced below about 8 km, and reduced above. However, the effect is more pronounced during summer related to larger photochemical activity. In particular, there is no reduction in chemical ozone production in the Arctic lower stratosphere during the winter season.

A normalized scenario for the lower flight altitude case was created to estimate the effect from changes in fuel consumption individually. Lowering the cruise altitude will increase air resistance because the air density increases with decreasing altitude in the atmosphere. As a result, fuel consumption and NO$_x$ emissions will increase. Figure 11 shows the separate effect of increasing fuel emission along with the total effect of reducing flight altitude on zonal-mean ozone. Although the magnitude of changes related to fuel consumption is much smaller than the total aircraft effect, it has to be noted that the increase covers all altitudes, i.e. there are no canceling effects between changes of opposite signs at different altitudes. Therefore, in terms of total ozone change, the effect of increased fuel burn is large compared to the effect from lowering the flight altitude alone.
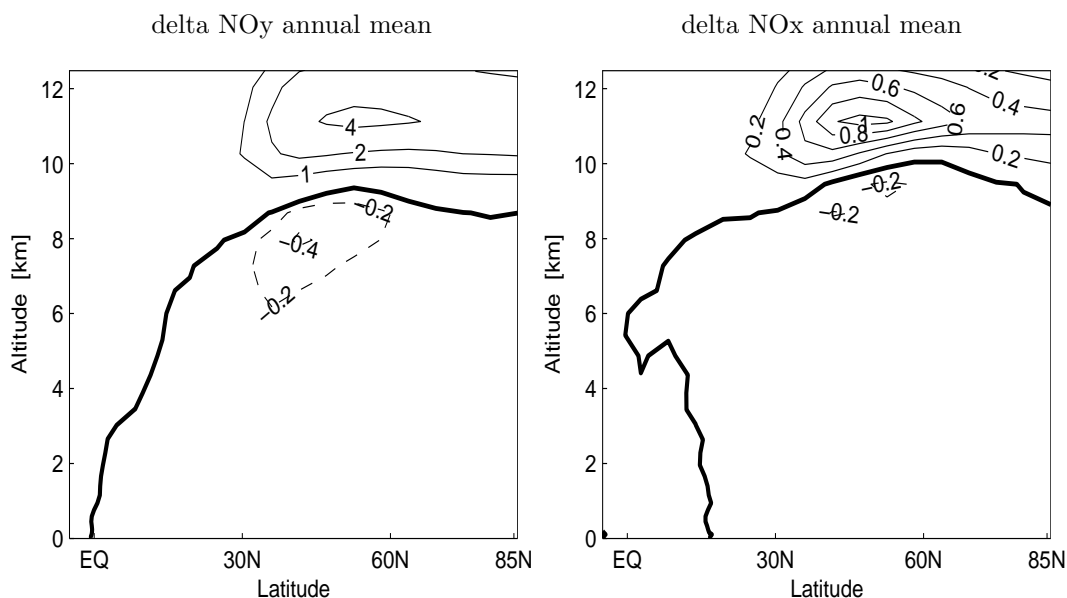
delta NOy annual mean

delta NOx annual mean

Fig. 12. Annual-mean changes in concentrations of NO$_y$ (top left, 10^8 molecules cm^{-3}) and NO$_x$ (top right, 10^8 molecules cm^{-3}) in the Northern Hemisphere due to a 610 m increase in flight altitude taking into account changes in the total emission of nitrogen, i.e."high_adj minus base". Contours at –0.4, –0.2, 0, 1, 2, 4 for NO$_y$ and –0.4, –0.2, 0, 0.2, 0.4, 0.6, 0.8, 1.0 for NO$_x$.
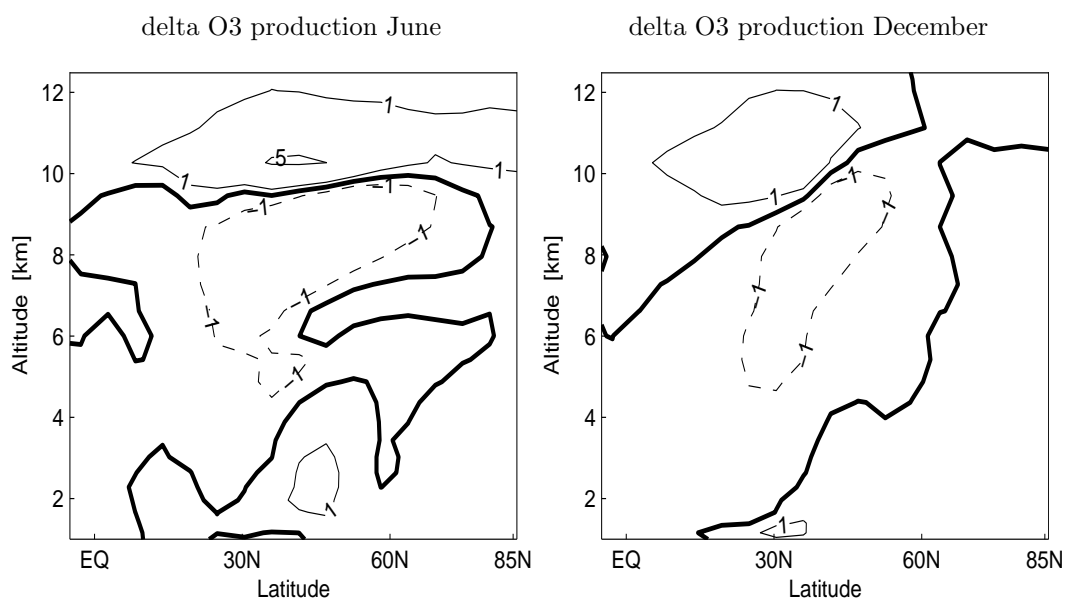
delta O3 production June

delta O3 production December

Fig. 13. Change in net chemical ozone production (10^3 molecules cm^{-3} s^{-1}) due to a 610 m increase in flight altitude, taking into account changes in the total emission of nitrogen, i.e."high_adj minus base" in June (left) and December (right). Contours at –5, –1, 0, 1, 5.

As shown in Table 3, the total increase in the "base" case is +0.339 DU (+3.71 Tg). Reducing flight altitude alone ("low_norm minus base") leads to a decrease of –0.0266 DU (–0.29 Tg) and increasing fuel use ("low_adj minus low_norm") to +0.0131 DU (+0.14 Tg), so that the total increase due to aircraft in the lower flight altitude scenario ("low_adj minus no_air") amounts to +0.3255 DU

(+3.56 Tg). These findings are in qualitative agreement with the results in a similar study of Grewe et al. (2002b), while the magnitudes of change cannot easily be compared because of the larger total emission from aircraft and the smaller altitude decrease considered in the Grewe et al. study. Also, it has to be noted that the effect on column ozone is strongly dependent on both season and latitude, as reflected by the
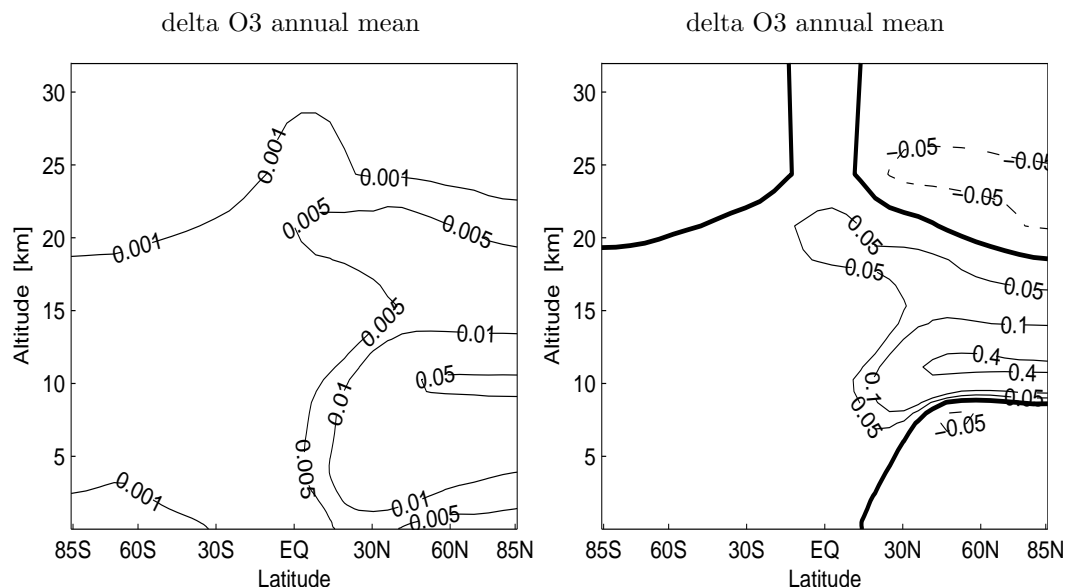
delta O3 annual mean   delta O3 annual mean

Fig. 14. Annually averaged zonal-mean ozone change (ppbv) due a 610 m increase in flight altitude. Left panel: "high_adj minus high_norm", i.e. separated effect of changes in fuel consumption, and right panel: "high_adj minus base", i.e. total effect of increasing the flight altitude.

varying gap between the green dotted and the solid black lines in Fig. 8 (lower panel) and the latitudinal distribution of total ozone change (not shown). The reduction in flight altitude leads to decreases in the tropospheric ozone column in low latitudes, which is a clear manifestation of the importance of washout processes. Both in the "base" case and in the lower-altitude case, virtually all low-latitude aircraft traffic is located in the troposphere, and the lowering of the aircraft emission source results in a larger fraction of emitted nitrogen emissions to be washed out. In contrast, an increase in the tropospheric ozone column is modeled at mid- to high Northern latitudes for the lower-altitude scenario ("low_adj"). This is due to the enhanced fuel use, and the larger fraction emitted in the troposphere with respect to the "base" case. However, this increase is overcompensated by a corresponding stratospheric decrease during summer and mid-winter so that the total ozone column change is negative in these seasons, as it is in all seasons at low latitudes. During summer the main reason for this is the high tropopause. A large fraction of aircraft emissions is occurring in the troposphere so that the increase of washout processes and the decrease of ozone lifetime with decreasing altitude are important. On the other hand, during spring and autumn the tropopause tends to be lower and even in the low altitude scenario a very large fraction of aircraft emissions occurs in the stratosphere, where washout does not play a role. The other effect, i.e. the decrease in residence times of pollutants in the lower stratosphere with decreasing altitude is not sufficiently important to compensate for the increases in the troposphere. The effect on the total column is thus positive, albeit only slightly. The next option, an increase in

flight altitude by 610 m, is investigated through model runs "high_norm" and "high_adj". Figure 12 shows annually averaged zonal-mean changes in the concentrations of NO$_y$ and NO$_x$ due to a 610 m increase in flight altitude taking into account changes in fuel consumption and in the total emission of nitrogen. In Northern mid- to high latitudes we calculate increases above 8 to 9 km altitude and decreases below. Again, the effect at high altitudes is larger in magnitude than the effect at low altitudes. For instance, the maximum (high altitude) increase in NO$_y$ amounts to $+4.5 \times 10^8$ molecules, while the magnitude of the largest reduction is about ten times smaller, -0.43×10^8 molecules/cm^3. This can be in part explained by less efficient washout of excess NO$_y$ at the new (and higher) altitude of emission. Also, the longer effluent lifetime at higher altitudes allows for more pronounced increases and thereby to increased downward flux of NO$_y$, which partly compensates for the reduced in situ NO$_x$ emissions at lower altitudes. Maximum changes in NO$_x$ and NO$_y$ are displayed in Fig. 8. Slightly larger perturbations are obtained compared to the "base" case, with the fuel consumption effect being of minor importance.

By and large, increases of the OH/HO$_2$ ratio (not shown) are seen in regions where the NO$_x$ emission is enhanced, while reductions in NO$_x$ emissions are marked by lower OH and higher HO$_2$ concentrations. Qualitatively, the effect of higher flight altitude is approximately opposite from what is obtained in the lower-altitude simulations. However, the magnitude of the effect is somewhat smaller, primarily because the change in flight altitude is smaller. The same is true for changes in the chemical net production, which is shown in Fig. 13. The tendency is a reduction below about 8 to
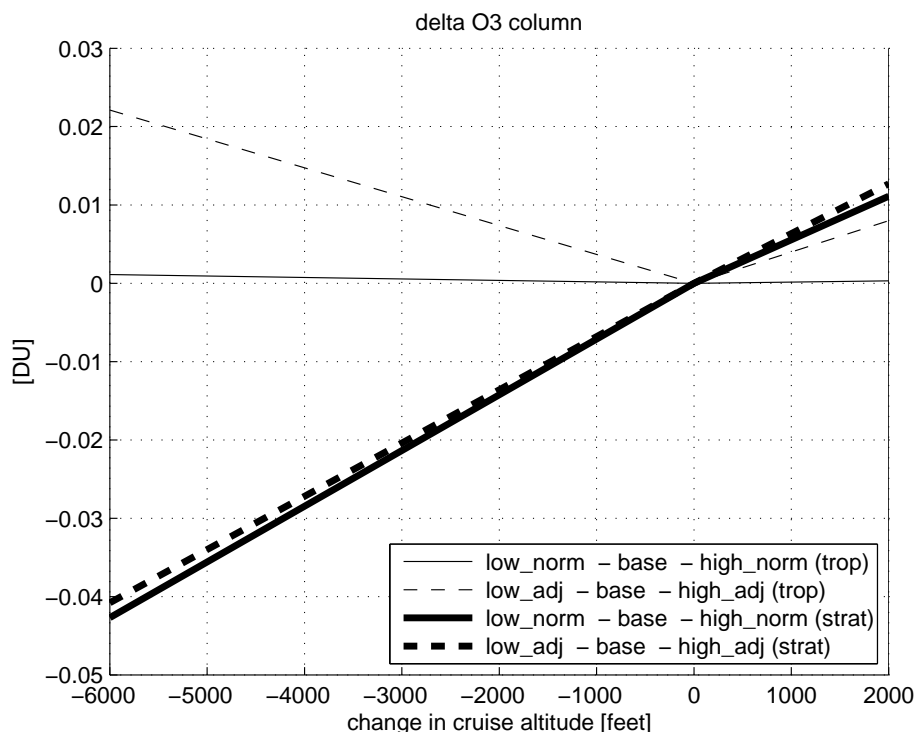
Fig. 15. Change in the Northern Hemisphere average tropospheric and stratospheric ozone columns (DU) due to changes in flight altitude, based on the numbers given in Table 4. The increase in the "base" run is set to zero. E.g., the thin dashed line depicts the 0.0221 DU increase in tropospheric ozone column in simulation "low_adj" with respect to "base" (at –6000 feet) and the 0.0080 DU increase in the tropospheric ozone column in simulation "high_adj" with respect to "base" (at +2000 feet).

10 km, and an enhancement above, which is again most pronounced during summer, as it was in the lower-altitude case (Fig. 10).

Figure 14 shows the individual effect of changes in fuel consumption and the overall effect of increasing the flight altitude on zonal-mean ozone. The effect of the increased NO$_x$ emissions from fuel burn enhancement is positive at all altitudes, while the overall effect is slightly negative at low altitudes, positive in the lower stratosphere and again negative in the middle stratosphere, probably due to ozone depletion mechanisms involving NO$_x$, which is increased at this altitude with respect to the "base" case run. As seen in Table 3 the overall effect on the ozone column due to increased flight altitude is positive both in the stratosphere and in the troposphere. Through the increase in flight altitude the ozone increase is enhanced by 0.0103 DU (0.11 Tg) globally ("high_adj minus base"), while the increase in NO$_x$ emission due to the higher E.I.(NO$_x$) contributes another 0.0054 DU (0.06 Tg) ("high_adj minus high_norm"), so that the overall effect increase represented by the difference "high_adj minus base" amounts to 0.0157 DU (0.17 Tg). Averaged over the Northern Hemisphere the increase equals 0.0207 DU, corresponding to a 0.11 Tg increase of the hemispheric burden.

The effect on the globally averaged ozone column is depicted by the red lines in Fig. 8 (bottom panel). Concern-

ing the latitudinal and seasonal variation of ozone column change (not shown), the results are, by and large, opposite in sign to what is obtained for a reduction in flight altitude. In the Southern Hemisphere and in low latitudes of the Northern Hemisphere, there is an increase in both the tropospheric and the stratospheric columns. In mid- to high latitudes the effect on the tropospheric column is negative because of the relatively low tropopause causing a large reduction in tropospheric emissions in the high-altitude scenario. By contrast, due to the high summer tropopause a large fraction of emission occurs in the troposphere even in the high altitude scenario allowing for increases in the ozone impact related to less efficient washout of pollutants. The effect of enhanced flight altitudes on the total ozone column is positive almost everywhere, except for high Northern latitudes in December. As this exception occurs in the absence of sunlight, it must be related to transport of air that is poorer in ozone compared to the "base" case.

In Fig. 15 the dependence of changes in tropospheric and stratospheric ozone columns on flight altitude is visualized relative to the changes calculated for the "base" case. The perturbations due to a 6000-feet reduction in flight altitude are positive for the tropospheric and negative for the stratospheric ozone columns, which is a consequence of increased tropospheric and reduced stratospheric emissions,

respectively. The increase in tropospheric columns is much more pronounced when the increased fuel emission is taken into account.

A 2000-feet increase in flight altitude leads to increases in both the tropospheric and the stratospheric ozone column. Increases in the stratosphere are a direct consequence of increased emissions, while increases in the troposphere are mostly due to increased downward transport of NO$_y$ and resulting increases in tropospheric ozone production.

5 Conclusions and future directions

In this paper we have presented results from an extensive model study performed for the TRADEOFF project focusing on the environmental impact of aircraft emissions and options to reduce the impact for present conditions (year 2000) and on the impact of aircraft emissions in a future (year 2050) atmosphere. We have used a 3-D chemical transport model including comprehensive chemistry schemes for the troposphere and the stratosphere in order to take into account all chemical processes relevant for the UTLS.

In agreement with earlier studies, substantial perturbations in NO$_y$ and NO$_x$ are modeled in the tropopause region of the Northern Hemisphere with a strong zonal variability in the case of NO$_x$. The resulting maximum perturbations in zonal-mean ozone range between about 3 and 8 ppbv, depending on season.

Emission scenarios regarding enhanced use of polar routes result in substantially enhanced increase in polar stratospheric ozone. However, this increase is confined to the summer season. Judging by ozone changes only, the aircraft impact could thus be reduced by enhanced use of high latitude routes during winter.

This study has also investigated the impact of changes in flight altitude based on realistic aircraft emission scenarios. Changes in flight altitude modify the vertical profile of ozone changes. In terms of annually averaged total ozone column change, an increase in flight altitude leads to a larger impact, while a reduction in flight altitude leads to a smaller impact than in the scenario assuming standard flight altitudes. However, these effects are highly dependent on season, latitude, and local meteorological conditions. In mid- to high Northern latitudes during summer, lowering the flight altitude significantly reduces the aircraft impact on ozone, while in spring and autumn, larger ozone column increases are modeled. Increasing the flight altitude is calculated to result in larger total ozone increases in all seasons and latitudes, with the exception of high Northern latitudes in late autumn in the absence of sunlight.

Aircraft-induced changes in ozone and modifications in the height profile of ozone change will alter radiative forcing exerted by ozone. Radiative forcing calculations are being performed based on the ozone perturbations discussed in this paper and changes in methane lifetime calculated by the CTM2 (G. Myhre, University of Oslo, personal communication) and will be published in the near future by Stordal et al. (2006)[1]. In addition, it is planned to run the CTM on a higher horizontal resolution and with meteorology from other years than 2000 (in order to assess the inter-annual variation of the impact), to include PAN and acetone chemistry explicitly in the stratospheric chemistry package, and chlorine chemistry in the tropospheric module.

In terms of the potential climate impact from aircraft, it has to be noted that this study only deals with changes in ozone and methane. In order to make practical suggestions on how to reduce aircraft impact by changes in flight altitude and routing, these results have to be considered in connection with other aspects of aircraft impact on the environment. For example, changes in flight routing will, in general, lead to changes in fuel consumption and thus in emissions of CO$_2$, a major greenhouse gas. This effect will also be taken into account in the above mentioned Stordal et al. (2006) publication. Contrails and cirrus clouds constitute another important climate impact from aircraft (e.g. Marquart et al., 2003; Isaksen et al., 2003). Their formation is largely controlled by the ambient meteorological conditions including pressure and humidity and therefore is strongly dependent on flight altitude and latitude (Fichter et al., 2005). The resulting radiative forcing depends on their optical properties, solar zenith angle, and natural cloud cover, all of which need to be modeled accurately.

Following an integrated analysis of all aspects of aircraft impact for different atmospheric conditions and options for flight routing, suggestions on how to reduce the environmental impact have to be examined together with safety considerations and air traffic restrictions before decisions can be taken. The present study has thus to be viewed as one important input to the overall assessment of the environmental impact of civil aviation.

References

Airbus, S. A. S.: Global Market Forecast, 31 707 BLAGNAC CEDEX, France, Reference CB 390.0008/02, 2002.

---

[1]Stordal, F., Myhre, G., Gauss, M., et al.: TRADEOFFs in climate effects through aircraft routing: Forcing due to radiatively active gases, in preparation, 2006.

Berntsen, T. and Isaksen, I. S. A.: A global 3-D chemical transport model for the troposphere, 1, Model description and CO and Ozone results, J. Geophys. Res., 102(D23), 21 239–21 280, 1997.

Berntsen, T. K. and Isaksen, I. S. A.: Effects of lightning and convection on changes in upper tropospheric ozone due to aircraft, Tellus, 51B, 766–788, 1999.

Bian, H. S. and Prather, M. J.: Fast-J2: Accurate simulation of stratospheric photolysis in global chemical models, J. Atmos. Chem., 41(3), 281–296, 2002.

Brasseur, G., Cox, R., Hauglustaine, D., Isaksen, I. S. A., Lelieveld, J., Lister, D., Sausen, R., Schumann, U., Wahner, A., and Wiesen, P.: European scientific assessment of the atmospheric effect of aircraft emissions, Atmos. Environ., 32, 2329–2418, 1998.

Bregman, A., Krol, M. C., Teyssedre, H., Norton, W. A., Iwi, A., Chipperfield, M. Pitari, G., Sundet, J. K., and Lelieveld, J.: Chemistry-transport model comparison with ozone observation in the midlatitude lowermost stratosphere, J. Geophys. Res., 106(D15), 17 479–17 489, 2001.

Brühl, C., Pöschl, U., Crutzen, P., and Steil, B.: Acetone and PAN in the upper troposphere: Impact on ozone production from aircraft emissions, Atmos. Environ., 34, 3931–3938, 2000.

Brunner, D., Staehelin, J., Rogers, H. L., Köhler, M. O., Pyle, J. A., Hauglustaine, D. A., Jourdain, L., Berntsen, T. K., Gauss, M., Isaksen, I. S. A., Meijer, E., van Velthoven, P., Pitari, G., Mancini, E., Grewe, V., and Sausen, R.: An evaluation of the performance of chemistry transport models by comparison with research aircraft observations, Part 1, Concepts and overall model performance, Atmos. Chem. Phys., 3, 1609–1631, 2003.

Brunner, D., Staehelin, J., Rogers, H. L., Köhler, M. O., Pyle, J. A., Hauglustaine, D. A., Jourdain, L., Berntsen, T. K., Gauss, M., Isaksen, I. S. A., Meijer, E., van Velthoven, P., Pitari, G., Mancini, E., Grewe, V., and Sausen, R.: An evaluation of the performance of chemistry transport models – Part 2: Detailed comparison with two selected campaigns, Atmos. Chem. Phys., 5, 107–129, 2005.

Carslaw, K., Luo, B., and Peter, T.: An analytic expression for the composition of aqueous HNO3+H2SO4 stratospheric aerosols including gas phase removal of HNO3, Geophys. Res. Lett., 22(14), 1877–1880, 1995.

Crutzen, P. J.: The influence of nitrogen oxides on atmospheric ozone content, Q. J. R. Meteorol. Soc., 96, 320–325, 1970.

Dameris, M., Grewe, V., Köhler, I., Sausen, P., Bruehl, C., Grooss, J., and Steil, B.: Impact of aircraft NO$_x$ emissions on tropospheric and stratospheric ozone, Part II, 3D model results, Atmos. Environ., 32, 3185–3199, 1998.

DeMore, W. G., Sander, S. P., Golden, D. M., Hampson, R. F., Kurylo, M. J., Howard, C. J., Ravishankara, A. R., Kolb, C. E., and Molina, M. J.: Chemical Kinetics and Photochemical Data for Use in Stratospheric Modeling, Evaluation No. 12, JPL Publication 97-4, Jet Propulsion Laboratory, Pasadena, CA, 1997.

Fabian, P. and Kärcher, B.: The impact of aviation upon the atmosphere, Phys. Chem. Earth, 22, 503–598, 1997.

FESG: Report of the Forecasting and Economic Support Group to CAEP/4, International Civil Aviation Organization Committee on Aviation Environmental Protection, Montreal Canada, 6–8 April 1998, 132, 1998.

Fichter, C., Marquart, S., Sausen, R., and Lee, D. S.: The impact of cruise altitude on contrails and related radiative forcing, Meteorol. Z., 14(4), 563–572, 2005.

Gardner, R. M., Adams, K., Cook, T., Ernedal, S., Falk, R., Fleuti, E., Herms, E., Johnson, C. E., Lecht, M., Lee, D. S., Leech, M., Lister, D., Massé, B., Metcalfe, M., Newton, P., Schmitt, A., Vandenbergh, C., and van Drimmelen R.: The ANCAT/EC global inventory of NO$_x$ emissions from aircraft, Atmos. Env., 31, 1751–1766, 1997.

Gardner, R. M., Adams, J. K., Cook, T., Lason, L. G., Falk, R. S., Fleuti, E., Förtsch, W., Lecht, M., Lee, D. S., Leech, M. V., Lister, D. H., Massé, B., Morris, K., Newton, P. J., Owen, A., Parker, E., Schmitt, A., ten Have, H., and Vandenbergh, C.: ANCAT/EC2 Global Aircraft Emission Inventories for 1991/92 and 2015, Report by the ECAC/ANCAT and EC working group, EUR-18179, 1998.

Gauss, M., Isaksen, I. S. A., Wong, S., and Wang, W.-C.: Impact of H2O emissions from cryoplanes and kerosene aircraft on the atmosphere, J. Geophys. Res., 108(D10), 4304, doi:10.1029/2002JD002623, 2003a.

Gauss, M., Myhre, G., Pitari, G., Prather, M. J., Isaksen, I. S. A., Berntsen, T. K., Brasseur, G. P., Dentener, F. J., Derwent, R. G., Hauglustaine, D. A., Horowitz, L. W., Jacob, D. J., Johnson, M., Law, K. S., Mickley, L. J., Müller, J.-F., Plantevin, P.-H., Pyle, J. A., Rogers, H. L., Stevenson, D. S., Sundet, J. K., van Weele, M., and Wild, O.: Radiative forcing in the 21st century due to ozone changes in the troposphere and the lower stratosphere, J. Geophys. Res., 108(D9), doi:10.1029/2002JD002624, 2003b.

Gauss, M., Myhre, G., Isaksen, I. S. A., Grewe, V., Pitari, G., Wild, O., Collins, W. J., Dentener, F. J., Ellingsen, K., Gohar, L. K., Hauglustaine, D. A., Iachetti, D., Lamarque, J.-F., Mancini, E., Mickley, L. J., Prather, M. J., Pyle, J. A., Sanderson, M. G., Shine, K. P., Stevenson, D. S., Sudo, K., Szopa, S., and Zeng, G.: Radiative forcing since preindustrial times due to ozone change in the troposphere and the lower stratosphere, Atmos. Chem. Phys., 6, 575–599, 2006.

Gettelman, A. and Baughcum, S.: Direct deposition of subsonic aircraft emissions into the stratosphere, J. Geophys. Res., 104(D7), 8317–8327, 1999.

Grewe, V., Dameris, M., Fichter, C., and Sausen, R.: Impact of aircraft NO$_x$ emissions. Part 1: Interactively coupled climate-chemistry simulations and sensitivities to climate-chemistry feedback, lightning and model resolution, Meteorol. Z., 11(3), 177–186, 2002a.

Grewe, V., Dameris, M., Fichter, C., and Lee, D. S.: Impact of aircraft NO$_x$ emissions. Part 2: Effects of lowering the flight altitude, Meteorol. Z., 11(3), 197–205, 2002b.

Grini, A., Myhre, G., Sundet, J. K., and Isaksen, I. S. A.: Modeling the annual cycle of sea salt in the global 3-D model Oslo CTM-2, concentration, fluxes and radiative impact, J. Clim., 15, 1717–1730, 2002.

Hansen, J., Sato, M., and Ruedy, R.: Radiative forcing and climate response, J. Geophys. Res., 102(D6), 6831–6864, 1997.

Henderson, S. C., Wickrama, U. K., Baughcum, S. L., Begin, J. L., Franco, F., Greene, D. L., Lee, D. S., Mclaren, M. L., Mortlock, A. K., Newton, P. J., Schmitt, A., Sutkus, D. J., Vedantham, A., and Wuebbles, D. J.: Aircraft emissions: current inventories and future scenarios, Chapter 9 of "Aviation and the Global Atmosphere", edited by: Penner, J. E., Lister, D. H., Griggs, D. J., Dokken, D. J., and McFarland, M., Special Report of the

Intergovernmental Panel on Climate Change, Cambridge University Press, Cambridge, UK, 1999.

Hesstvedt, E., Hov, O., and Isaksen, I. S. A.: Quasi steady-state approximation in air pollution modelling, Comparison of two numerical schemes for oxidant prediction, Int. J. Chem. Kinetics, X, 971–994, 1978.

Hidalgo, H. and Crutzen, P. J.: The tropospheric and stratospheric composition perturbed by NO$_x$ emissions of high-altitude aircraft, J. Geophys. Res., 82, 5833–5866, 1977.

Holtslag, A. A. M., DrBruijn, E. I. F., and Pan, H.-L.: A High resolution air mass transformation model for short-range weather forecasting, Mon. Wea. Rev., 118, 1561–1575, 1990.

Isaksen, I. S. A., Rognerud, B., Stordal, F., Coffey, M. T., and Mankin, W. G.: Studies of Arctic stratospheric ozone in a 2-d model including some effects of zonal asymmetries, Geophys. Res. Lett., 17, 557–560, 1990.

Isaksen, I. S. A., Berntsen, T. K., and Wang, W.-C.: NO$_x$ Emissions from Aircraft: Its Impact on the Global Distribution of CH4 and O3 and on Radiative Forcing, Terrestrial, Atmos. Ocean. Sci., 12, 1, 63–78, 2001.

Isaksen, I. S. A., Sausen, R., Pyle, J. A., et al.: The EU project TRADEOFF – Aircraft emissions: Contributions of various climate compounds to changes in composition and radiative forcing – tradeoff to reduce atmospheric impact, Project Final report, Contract No. EVK2-CT-1999-0030 (available from the Department of Geosciences, University of Oslo, Oslo, Norway), 158, 2003.

Isaksen, I. S. A., Zerefos, C., Kourtidis, K., Meleti, C., Dalsoren, S. B., Sundet, J. K., Grini, A., Zanis, P., and Balis, D.: Tropospheric ozone changes at unpolluted and semipolluted regions induced by stratospheric ozone changes, J. Geophys. Res., 110(D2), doi:10.1029/2004JD004618, 2005.

Jaeglé, L., Jacob, D. J., Brune, W. H., Tan, D., Faloona, I. C., Weinheimer, A. J., Ridely, B. A., Campos, T. L., and Sachse, G. W.: Sources of HO$_x$ and ozone production in the upper troposphere over the United States, Geophys. Res. Lett., 25(10), 1709–1712, 1998.

Jaeglé, L., Jacob, D. J., Brune, W. H., Faloona, I. C., Tan, D., Kondo, Y., Sachse, G. W., Anderson, B., Gregory, G. L., Vay, S., Singh, H. B., Blake, D. R., and Shetter, R.: Ozone production in the upper troposphere and the influence of aircraft during SONEX, Approach of NO$_x$-saturated conditions, Geophys. Res. Lett., 26(20), 3081–3084, 1999.

Johnson, C. E., Henshaw, J., and McInnes, G.: Impact of aircraft and surface emissions of nitrogen oxides on tropospheric ozone and global warming, Nature, 355, 69–71, 1992.

Johnston, H. S.: Reduction of stratospheric ozone by nitrogen oxide catalysts from supersonic transport exhaust, Science, 173, 517–522, 1971.

Kentarchos, A. S. and Roelofs, G. J.: Impact of aircraft NO$_x$ emissions on tropospheric ozone calculated with a chemistry-general circulation model, Sensitivity to higher hydrocarbon chemistry, J. Geophys. Res., 107(D13), doi:10.1029/2001JD000828, 2002.

Köhler, I., Sausen, R., and Reinberger, R.: Contribution of aircraft emissions to the atmospheric NO$_x$ content, Atmos. Environ., 31, 1801–1818, 1997.

Kraabøl, A. G., Stordal, F., Konopka, P., and Knudsen, S.: The NILU aircraft plume model: A technical description, NILU Tech. Rep., TR 4/99, Norwegian Institute for Air Research, Nor-

way, 1999.

Kraabøl, A. G., Berntsen, T. K., Sundet, J. K., and Stordal, F.: Impacts of NO$_x$ emissions from subsonic aircraft in a global three dimensional chemistry transport model including plume processes, J. Geophys. Res., 107(D22), doi:10.1029/2001JD001019, 2002.

Lacis, A. A., Wuebbles, D. J., and Logan, J. A.: Radiative forcing by changes in the vertical distribution of ozone, J. Geophys. Res., 95, 9971–9981, 1990.

Lee, D. S., Köhler, I., Grobler, E., Rohrer, F., Sausen, R., Gallardo-Klenner, L., Olivier, J. J. G., and Dentener, F. D.: Estimations of global NO$_x$ emissions and their uncertainties, Atmos. Environ., 31, 1735–1749, 1997.

Lee, D. S., Owen, B., Graham, A., Fichter, C., Lim, L. L. and Dimitriu, D.: Allocation of International aviation emissions from scheduled air traffic – present day and historical (Report 2 of 3), Manchester Metropolitan University, Centre for Air Transport and the Environment, CATE-2005-3(C)-2, Manchester, UK, 2005.

Leggett, J., Pepper, W. J., and Swart, R. J.: Emissions scenarios for the IPCC: an update, in: Climate Change 1992: The Supplementary Report to the IPCC Scientific Assessment, prepared by: IPCC Working Group I (edited by: Houghton, J. T., Callander, B. A., and Varney, S. K.) and WMO/UNEP, Cambridge University Press, Cambridge, UK, and New York, NY, USA, 1992.

Marquart S., Ponater, M., Mager, F., and Sausen, R.: Future development of contrail cover, optical depth, and radiative forcing: Impacts of increasing air traffic and climate change, J. Clim., 16(17), 2890–2904, 2003.

Müller, J. F.: Geographical distribution and seasonal variation of surface emissions and deposition velocities of atmospheric trace gases, J. Geophys. Res., 97, 3787–3804, 1992.

Olivier, J. G. J., Bouwman, A. F., Berdowski, J. J. M., Veldt, C., Bloos, J. P. J., Visschedijk, A. J. H., van der Maas, C. W. M., and Zasndveld, P. Y. J.: Sectoral emission inventories of greenhouse gases for 1990 on a per country basis as well as on 1×1, Environ. Sci. Policy, 2, 241–263, 1999.

Penner, J. E., Lister, D. H., Griggs, D. J., Dokken, D. J., and McFarland, M.: Aviation and the Global Atmosphere. A special report of IPCC Working Groups I and III, 373, Cambridge Univ. Press, Cambridge, UK, 1999.

Pickering, K. E., Wang, Y. S., Tao, W. K., Price, C., and Müller, J. F.: Vertical distributions of lightning NO$_x$ for use in regional and global chemical transport models, J. Geophys. Res., 103(D23), 31 203–31 216, 1998.

Prather, M. J.: Numerical advection by conservation of second-order moments, J. Geophys. Res., 91, 6671–6681, 1986.

Prather, M. J.: Lifetimes and eigenstates in atmospheric chemistry, Geophys. Res. Lett., 21(9), 801–804, 1994.

Prather, M., Ehhalt, D., Dentener, F., Derwent, R., Dlugokencky, E., Holland, E., Isaksen, I., Katima, J., Kirchhoff, V., Matson, P., Midgley, P., and Wang, M.: Atmospheric Chemistry and Greenhouse Gases, in: Climate Change 2001, the Scientific Basis, Contribution of Working Group I to the Third Assessment Report of the Intergovernmental Panel on Climate Change (IPCC), edited by: Houghton, J. T., Ding, Y., Griggs, D. J., Noguer, M., van der Linden, P. J., Dai, X., Maskell, K., and Johnson, C. A., Cambridge University Press, Cambridge, UK and New York, NY, USA, 881, 2001.

Price, C., Penner, J., and Prather, M.: NO$_x$ from lightning 1. Global distribution based on lightning physics, J. Geophys. Res., 102(D5), 5929–5942, 1997a.

Price, C., Penner, J., and Prather, M.: NO$_x$ from lightning 2. Constraints from the global atmospheric circuit, J. Geophys. Res., 102(D5), 5943–5952, 1997b.

Ramaswamy, V., Boucher, O., Haigh, J., Hauglustaine, D., Haywood, J., Myhre, G., Nakajima, T., Shi, G. Y., and Solomon, S.: Radiative Forcing of Climate Change, in: Climate Change 2001, The Scientific Basis, Contribution of Working Group I to the Third Assessment Report of the Intergovernmental Panel on Climate Change (IPCC), edited by: Houghton, J. T., Ding, Y., Griggs, D. J., Noguer, M., van der Linden, P. J., Dai, X., Maskell, K., and Johnson, C. A., Cambridge University Press, Cambridge, UK and New York, NY, USA, 881, 2001.

Rummukainen, M., Isaksen, I. S. A., Rognerud, B., and Stordal, F.: A global model tool for three-dimensional multiyear stratospheric chemistry simulations: Model description and first results, J. Geophys. Res., 104(D21), 26 437–26 456, 1999.

Sander, S. P., Friedl, R. R., DeMore, W. B., Golden, D. M., Kurylo, M. J., Hampson, R. F., Huie, R. E., Moortgat, G. K., Ravishankara, A. R., Kolb, C. E., and Molina, M. J.: Chemical Kinetics and Photochemical Data for Use in Stratospheric Modeling, Evaluation No. 13, JPL Publication 00-3, Jet Propulsion Laboratory, Pasadena, CA, 2000.

Schumann, U.: The impact of nitrogen oxides emissions from aircraft upon the atmosphere at flight altitudes – Results from the AERONOX project, Atmos. Environ., 31, 1723–1733, 1997.

Schumann, U., Schlager, H., Arnold, F., Ovarlez, J., Kelder, H., Hov, Ø., Hayman, G., Isaksen, I., Staehelin, J., and Whitefield, P.: Pollution from aircraft emissions in the North Atlantic Flight Corridor, Overview on the POLINAT projects, J. Geophys. Res., 105(D3), 3605–3631, 2000.

Stevenson, D., Collins, W., Johnson, C., and Derwent, R.: The impact of aircraft nitrogen oxide emissions on tropospheric ozone studied with a 3D Lagrangian model including fully diurnal chemistry, Atmos. Environ., 31, 1837–1850, 1997.

Stevenson, D. S., Doherty, R. M., Sanderson, M. G., Collins, W. J., Johnson, C. E., and Derwent, R. G. : Radiative forcing from aircraft NO$_x$ emissions: Mechanisms and seasonal dependence, J. Geophys. Res., 109, D17307, doi:10.1029/2004JD004759, 2004.

Stevenson, D. S., Dentener, F. J., Schultz, M. G., Ellingsen, K., van Noije, T. P. C., Wild, O., Zeng, G., Amann, M., Atherton, C. S., Bell, N., Bergmann, D. J., Bey, I., Butler, T., Cofala, J., Collins, W. J., Derwent, R. G., Doherty, R. M., Drevet, J., Eskes, H. J., Fiore, A. M., Gauss, M., Hauglustaine, D. A., Horowitz, L. W., Isaksen, I. S. A., Krol, M. C., Lamarque, J.-F., Lawrence, M. G., Montanaro, V., Müller, J.-F., Pitari, G., Prather, M. J., Pyle, J. A., Rast, S., Rodriguez, J. M., Sanderson, M. G., Savage, N. H., Shindell, D. T., Strahan, S. E., Sudo, K., and Szopa, S.: Multi-model ensemble simulations of present-day and near-future tropospheric ozone, J. Geophys. Res., in press, 111, D08301, doi:10.1029/2005JD006338, 2006.

Stordal, F., Isaksen, I. S. A., and Horntvedt, K.: A diabatic circulation two-dimensional model with photochemistry, Simulations of ozone and long-lived tracers with surface sources, J. Geophys. Res., 90, 5757–5776, 1985.

Tiedtke, M.: A Comprehensive Mass Flux Scheme for Cumulus Parameterisation on Large Scale Models, Mon. Wea. Rev., 117, 1779–1800, 1989.

van Velthoven, P. F. J., Wauben, W. M. F., Kelder, H., Köhler, I., Sausen, R., and Rohrer, F.: The passive transport of NO$_x$ emissions from aircraft studied with a hierarchy of models, Atmos. Environ., 31, 1783–1799, 1997.

Wang, W.-C. and Sze, N. D.: Coupled effects of atmospheric N2O and O3 on the Earth's climate, Nature, 286, 589–590, 1980.

Wauben, W., van Velthoven, P., and Kelder, H.: A 3D chemistry transport model study of the changes in atmospheric ozone due to aircraft NO$_x$ emissions, Atmos. Environ., 31, 1819–1836, 1997.

Wesely, M. L.: Parameterization of surface resistances to gaseous dry deposition in regionalscale numerical models, Atmos. Environ., 23, 1293–1304, 1989.

World Meteorological Organization (WMO): Scientific assessment of ozone depletion, 1998, Global ozone research and monitoring project – Report 44, Geneva, Switzerland, 732, 1999.